Journal Pre-proof

Sleep and circadian rhythm disruption alters the lung transcriptome to predispose to viral infection

Lewis Taylor, Felix Von Lendenfeld, Anna Ashton, Harshmeena Sanghani, Simona Di Pretoro, Laura Usselmann, Maria Veretennikova, Robert Dallmann, Jane A. McKeating, Sridhar Vasudevan, Aarti Jagannath

PII: S2589-0042(22)02150-2

DOI: https://doi.org/10.1016/j.isci.2022.105877

Reference: ISCI 105877

To appear in: *ISCIENCE*

Received Date: 22 March 2022

Revised Date: 11 October 2022

Accepted Date: 21 December 2022

Please cite this article as: Taylor, L., Von Lendenfeld, F., Ashton, A., Sanghani, H., Di Pretoro, S., Usselmann, L., Veretennikova, M., Dallmann, R., McKeating, J.A, Vasudevan, S., Jagannath, A., Sleep and circadian rhythm disruption alters the lung transcriptome to predispose to viral infection, *ISCIENCE* (2023), doi: https://doi.org/10.1016/j.isci.2022.105877.

Sleep deprived mouse

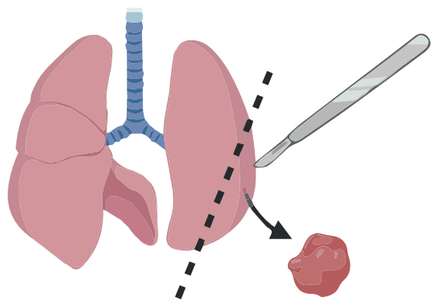

Lung tissue Transcriptomics

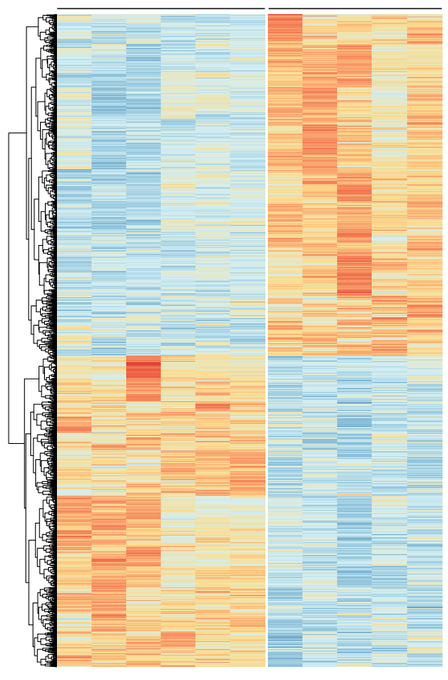

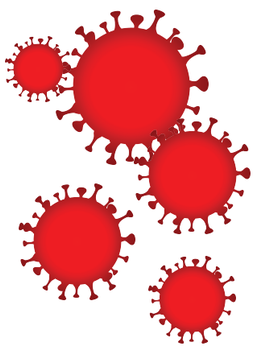

Shows increased susceptibility to viral infection

Sleep and circadian rhythm disruption alters the lung transcriptome to predispose to viral infection

Lewis Taylor[1], Felix Von Lendenfeld[1], Anna Ashton[1], Harshmeena Sanghani[2], Simona Di Pretoro[1], Laura Usselmann[3], Maria Veretennikova[4], Robert Dallmann[3], Jane A McKeating[5,6], Sridhar Vasudevan[2] and Aarti Jagannath[1]*

* Lead contact AJ (aarti.jagannath@ndcn.ox.ac.uk)

[1]Sleep and Circadian Neuroscience Institute (SCNi), Nuffield Department of Clinical Neurosciences, New Biochemistry Building, University of Oxford, South Parks Road, Oxford, OX1 3QU, U.K.

[2] Department of Pharmacology, University of Oxford, Mansfield Road, Oxford, OX1 3QT, U.K.

[3]Division of Biomedical Sciences, Warwick Medical School, Interdisciplinary Biomedical Research Building, Gibbet Hill Campus, University of Warwick, Coventry, CV4 7AL, UK

[4]Zeeman Institute for Systems Biology & Infectious Disease Epidemiology Research, Department of Mathematics, Mathematical Sciences Building, University of Warwick, Coventry, CV4 7AL, UK

[5]Nuffield Department of Medicine, University of Oxford, Old Road Campus, Oxford, OX3 7BN, UK.

[6]Chinese Academy of Medical Sciences (CAMS) Oxford Institute (COI), University of Oxford, Old Road Campus, Oxford, OX3 7BN, UK.

ABSTRACT

Sleep and circadian rhythm disruption (SCRD), as encountered during shift work, increases the risk of respiratory viral infection including SARS-CoV-2. However, the mechanism(s) underpinning higher rates of respiratory viral infection following SCRD remain poorly characterised. To address this, we investigated the effects of acute sleep deprivation on the mouse lung transcriptome. Here we show that sleep deprivation profoundly alters the transcriptional landscape of the lung, causing the suppression of both innate and adaptive immune systems, disrupting the circadian clock, and activating genes implicated in SARS-CoV-2 replication, thereby generating a lung environment that could promote viral infection and associated disease pathogenesis. Our study provides a mechanistic explanation of how SCRD increases the risk of respiratory viral infections including SARS-CoV-2 and highlights possible therapeutic avenues for the prevention and treatment of respiratory viral infection.

INTRODUCTION

Respiratory viral infections are among the leading causes of mortality worldwide and present a global medical and economic challenge [1,2]. Each year, billions of infections lead to millions of deaths, with the annual financial burden estimated at over $100 billion in the United States alone [3,4]. The recent emergence of severe acute respiratory syndrome coronavirus type 2 (SARS-CoV-2), the causative agent of COVID-19 [5], has highlighted the impact of respiratory viral infections, with more than 400 million SARS-CoV-2 infections and 5.7 million COVID-19 deaths to date (https://coronavirus.jhu.edu/map.html). An increased understanding of the risk factors and mechanisms driving severe respiratory disease will inform new treatment options. Sleep and circadian disruption have been reported to cause an increased risk of respiratory infections in mice and humans [6–10] and accumulating evidence suggests that shift work and the associated sleep deprivation and circadian rhythm misalignment are risk factors for COVID-19 [11–16]. Yet, a mechanistic explanation of how sleep and circadian disruption causes higher rates of viral infections remains to be determined.

The immune system is under tight sleep and circadian control. The circadian clock, a molecular transcriptional/translational feedback loop capable of aligning to the external day/night cycle [17,18], generates circadian rhythms; 24-hour oscillations in physiology and behaviour such as hormone secretion, metabolism, sleep, and immune function [19]. Indeed, leukocyte trafficking, host-pathogen interaction, and immune cell activation all display diurnal rhythms [20]. Furthermore, circadian differences in immune responses to vaccination, as well as a diverse range of pathogens and pathogen-derived products are well documented [21,22]. Immune responses to Influenza A, Hepatitis A and SARS-CoV-2 vaccines [23–25], and the infectivity of multiple viruses, including Influenza, is dependent on the time of virus challenge [26–29]. Disrupting the circadian system in experimental model systems has been reported to increase pro-inflammatory cytokine levels [30], and perturb immune cell function and trafficking [31]. Furthermore, it can promote the replication of a wide range of clinically important viruses including hepatitis B and C, Parainfluenza Virus Type 3, Respiratory Syncytial and Influenza A viruses, as shown in transgenic mouse models including BMAL1 KO animals [6,27,32–35], emphasising a central role of the circadian clock in regulating viral infection [36].

Sleep is one of the most essential circadian regulated behaviours; however, sleep and its homeostasis can be modified and disrupted independently from the circadian clock [37,38]. Sleep

disruption also leads to immune dysfunction, reducing natural killer cell activity [39], modifying pro-inflammatory cytokine production [40–43] and blood leukocyte numbers [44]. Importantly, sleep disruption impairs circadian and immune gene expression in multiple tissues [45], including the mouse brain [46], liver [47], and lung [48,49]. A similar disruption of the circadian clock and immune system is seen in blood samples from sleep deprived human subjects [50–52]. This dual sleep and circadian rhythm disruption (SCRD) is often encountered by shift workers, particularly those working at night, and is a well-established risk factor for respiratory viral infections. The common cold [53], Influenza [6,7,26], and indeed upper respiratory viral infections in general [8,10] are all significantly increased following SCRD. Notably, multiple recent studies have now found an association between shift work, sleep disruption and the risk of developing severe COVID-19. Rizza *et al.* established a significant association between SARS-CoV-2 infection and night shift work [54], and Rowlands *et al.* found that shift work increases the odds for severe COVID-19 twofold [15]. Alongside, Maidstone *et al.* observed that shift workers, regardless of their occupational group, are more likely to be hospitalised with severe COVID-19; even after adjusting for risk factors such as smoking history, obesity, and asthma [12]. This is consistent with the finding that people working night shifts irrespective of the job sector are 1.85 times more prone to SARS-CoV-2 infection [14]. Furthermore, a study on healthcare workers found that each extra hour of sleep reduces the risk for contracting COVID-19 by 12%, while workers reporting severe sleeping difficulties experience 88% higher odds of infection [16].

Despite the increased risk of respiratory viral infections in shift workers, and the established links between sleep, circadian rhythmicity and immune function, the molecular mechanism(s) underpinning higher rates of viral infection following SCRD remain poorly characterised. Therefore, we investigated the effects of acute sleep deprivation on the mouse lung transcriptome and host pathways known to be important for viral lifecycle. In particular we use SARS-CoV-2 as an exemplar, as the recent global research effort has provided a wealth of data detailing the molecular pathways regulating SARS-CoV-2 infectivity and the link between shift work and COVID-19 severity outcomes [55–58]. Here we show that 6 hours of sleep deprivation in mice profoundly alters the transcriptional architecture of the lung, with a majority of differentially expressed genes associated with host pathways that are essential for viral replication and a suppression of immune and circadian regulated genes with blunted circadian rhythmicity. Moreover, we found that SD causes the differential expression of several host factors implicated in SARS-CoV-2 infection, likely impacting SARS-CoV-2 entry, replication, and trafficking. Together, these data suggest that sleep deprivation alters the lung to provide an environment that could promote respiratory viral infection and pathogenesis.

RESULTS AND DISCUSSION

Acute sleep deprivation alters the lung transcriptome and dampens immune-associated gene expression.

To assess the effect of acute sleep deprivation on the lung transcriptome, RNA sequencing (RNA-Seq) was performed on lung tissue isolated from control (ad libitum sleep) or six-hour sleep deprived (SD) C57BL/6 mice (Fig. 1a). Gene expression analysis identified 2,366 upregulated and 2,157 downregulated transcripts following SD (Fig. 1b, c and Supplementary Table 1). We validated our RNA-Seq dataset using qRT-PCR and independent SD lung samples and observed highly correlated results for several top differential genes, confirming the robustness of our transcriptomic analysis (Supplementary Fig. 1). Gene ontology (GO)

biological pathway (BP) enrichment analysis of SD upregulated genes showed an enrichment in signal transduction (kinase activity and response to steroid hormones), as well as generic biological processes that are also implicated in viral entry and RNA replication, such as autophagy, Golgi organization, and cellular protein localization (Fig. 1d and Supplementary Table 2). Similar results were observed with Kyoto Encyclopaedia of Genes and Genomes (KEGG) pathway analysis of SD upregulated genes, highlighting protein processing in the ER, autophagy, and endocytosis (Fig. 1e and Supplementary Table 2). We also noted an enrichment for circadian rhythm genes (Fig. 1e - *Csnk1d, Cul1, Cry2, Csnk1e, Clock, Rora, Arntl, Npas2* and *Per1*). Analysis of the SD downregulated genes found that 215 GO BP terms were significantly enriched amongst the SD downregulated genes (adjusted p value < 0.01), with 154 (72%) comprising of immune system pathways. Of these, innate and adaptive immunity specific terms encompassed 18% and 23% respectively (Fig. 1f), suggesting that SD results in widespread immune depression in the lung. Indeed, multiple immune system pathways, including lymphocyte differentiation and proliferation, and leukocyte activation and migration, were repressed following acute SD (Fig. 1g and Supplementary Table 2). KEGG pathway analysis displayed a similar enrichment for immune associated terms in the SD downregulated gene population (Fig. 1h and Supplementary Table 2).

Cytokine production and chemokine signalling were also SD suppressed terms (Fig. 1g,h). Therefore we measured the levels of the inflammatory mediators TNF-α, IFN-γ, IL-6, and CCL5 in lung homogenates following acute SD to understand how our transcriptome data links to protein production. Alongside the reduced expression of *Ccl5* (Fig. 1i), we found a significant reduction in the abundance of CCL5 protein (Fig. 1j). Furthermore, multiple chemokine receptors, including *Ccr5* (the cognate receptor for CCL5), *Ccr2, Ccr3, Ccr6, Cxcr3, Cxcr5* and *Cx3cr1* were downregulated following SD, strongly suggesting that multiple aspects of chemokine signalling are impacted after SD. In order to examine how long this suppression of CCL5 persists, we measured lung CCL5 levels in animals allowed three hours of recovery sleep (RS) after SD. Notably, RS returned CCL5 to baseline levels (Supplementary Fig. 2) and suggests that the immune suppression caused by SD can be reversed once sleep is finally permitted.

In contrast, SD had no impact on *Tnf*, *Il6*, or *Ifng* transcript expression (Fig. 1i), which were all much lower than that of Ccl5, and resulted in no significant difference in TNF-α or IL-6 levels, and undetectable amounts of IFN-γ (Fig. 1j). Although these results appear to contradict the GO BP analysis that identified the regulation of TNF-α, IFN-γ and cytokine production (Fig. 1g), as the baseline level of IL-6 was very low, and IFN-γ undetectable (Fig. 1j), any impact on production could only be examined in light of a stimulus that would induce their expression. On the other hand, our data demonstrate that SD would decrease the ability of the immune system to respond to an inflammatory insult, and therefore the full impact of SD on a range of inflammatory processes, including mediator production, will only be unmasked in the face of an immune challenge, such as viral infection. Indeed, *Nfkbia*, a major negative regulator of pro-inflammatory transcription factor nuclear factor kappa (NF-κB), and *Tle1*, another NF-κB repressor, were upregulated after SD (Fig. 1k). Additionally, GO BP analysis revealed 12 SD upregulated genes implicated in the negative regulation of NF-κB, and 23 SD downregulated genes encoding positive regulators of NF-κB signalling (Supplementary Table 2); together suggesting that the NF-κB response would be blunted after infection. Similarly, leukocyte migration was also an SD downregulated process. The number of immune cells present in

bronchoalveolar lavage fluid is known to be very low under baseline conditions [59,60], but given the marked suppression of chemokine signalling detailed above, a deficit in leukocyte recruitment to the lung in sleep deprived mice would likely occur in response to an infectious insult.

Overall, these results suggest that sleep deprivation alters the lung transcriptome in a manner that would increase susceptibility to SARS-CoV-2 infection, and ideally, this would be confirmed with a study whereby animals are sleep deprived and then exposed to the virus and infectivity assessed. A limitation of this study is such an *in vivo* assessment was not carried out. In the absence of these data, a comparison with existing datasets of infected lungs to assess overlaps in differentially expressed genes presented an intermediary study that would support a future *in vivo* infection study. Therefore, to understand how the SD lung transcriptome compares to SARS-CoV-2 infection, we performed gene set enrichment analysis (GSEA) using the COVID-19 Drug and Gene Set Library [61] (Supplementary Table 3). When analysing the SD upregulated genes, the most significantly enriched gene set was the top 500 genes downregulated in the mouse lung three days post SARS-CoV-2 infection (3 DPI.), as determined by Li *et al.* [62] (Supplementary Fig. 3a). Indeed, there was a significant overlap between our SD upregulated genes and the top 500 downregulated genes 3 DPI (Supplementary Fig. 3b - Fisher's exact test p value = 7.7×10^{-26} and Supplementary Table 4). However, there was no such enrichment when comparing with the top 500 upregulated genes 3 DPI (Supplementary Fig. 3c). Conversely, when testing the SD downregulated genes, the most enriched gene set was the top 500 genes upregulated in the mouse lung 3 DPI (Supplementary Fig. 3d,e - Fisher's exact test p value = 8×10^{-37}), with no significant overlap with the downregulated 3 DPI (Supplementary Fig. 3f and Supplementary Table 4). In summary, the transcriptome of the lung following SD is inversely correlated with the lung transcriptome during early-stage SARS-CoV-2 infection. This suggests that SD skews the lung transcriptome away from that needed for mounting an anti-viral response, therefore predisposing towards infection. Indeed, *Furin*, which cleaves the SARS-CoV-2 spike protein and regulates particle entry [63], was upregulated following SD, whilst several Toll-like receptors (TLRs), which initiate innate immune responses, were all downregulated, including *Tlr3, Tlr7*, and *Tlr9* that have been shown to regulate COVID-19 pathogenesis [64,65] (Fig. 1i). Together, these findings suggest that in the lung, acute SD decreases the ability of the immune system to respond to infection by suppressing both the innate and adaptive immune arms and impacts multiple pathways important for viral host cell entry, intracellular replication, and trafficking.

Acute sleep deprivation dysregulates the circadian system in the lung

In order to understand what may be driving these gene expression changes in the lung, we analysed the transcriptome for the over-representation of transcription factor binding sites in the promoters of genes differentially regulated by SD. We found 757 significantly enriched transcription factor signatures (Supplementary Table 5), with regulators of immediate early genes (CREB1), and immune-associated genes (CEBPB, NFKB1, TCF7 and STAT3) highly represented (Supplementary Fig. 4). The question as to how much the lung transcriptome changes are actually due to stress should be addressed. Whilst the SD protocol we used induces relatively less corticosterone than others [66,67], stress and the activation of the HPA axis is unavoidable during SD [68], Therefore we analysed the transcriptome for NR3C1 binding sites in the promoters of genes differentially regulated by sleep deprivation and found that whilst NR3C1 was over-represented, it was not amongst the top 20 most over-represented

factors which included those specific to immune function such as TCF7, NFKB1 and STAT3, and the circadian clock (CLOCK). Therefore, stress is only a minor contributor towards the SD-induced changes in the lung transcriptome.

Notably, our over-representation analysis found that the core circadian transcription factor, CLOCK, was the most significantly enriched (Supplementary Fig. 4). As acute SD has also been previously reported to disrupt circadian rhythmic gene expression in multiple peripheral tissues [45,48,49,69], we therefore examined the how sleep deprivation impacts circadian processes in the lung. Rhythmic genes in the mouse lung were identified by sequencing the lung transcriptome at four time points throughout the day separated by 6-hour intervals (Zeitgeber time (ZT)2, ZT8, ZT14, and ZT20). We identified 2,029 significantly cycling genes in the mouse lung with a 24-hour period (JTK q-value < 0.05) (Fig. 2a and Supplementary Table 6). Interestingly, of these significantly cycling genes, 911 were also disrupted by SD, highlighting that almost 50% of rhythmic genes in the lung are SD sensitive (Fig. 2b and Supplementary Table 4). GO BP enrichment analysis of the 3,532 genes that were non-rhythmic, but SD-differential, revealed immune system associated terms such as leukocyte activation and migration (Fig. 2c and Supplementary Table 2), indicating that many of these immune genes were not circadian regulated, and instead were directly impacted by SD. Notably however, GO BP analysis of genes that were both rhythmic and SD-differential showed an enrichment for circadian regulation of gene expression, demonstrating that SD alters the circadian regulatory landscape of the lung (Fig. 2d and Supplementary Table 2). Pathways regulating metabolism, signalling, RNA processing, protein folding, and post-translational protein modification were also rhythmic and dysregulated following SD (Fig. 2d), suggesting a widespread disruption of normal circadian lung physiology. Indeed, several circadian transcripts were altered following SD; these included Bmal1 (*Arntl1*), *Clock, Per1, Cry2,* and *Rora* (Fig. 2e), suggesting that at this point of time (ZT6, post SD), the integrity of the core molecular circadian clock, and clock-controlled gene expression, was likely to be compromised.

This disruption to circadian rhythmicity could be examined by time course analysis of gene expression following sleep deprivation; however, all of the information needed to quantify circadian timing is contained in the phase relationships of different rhythmic genes in samples collected at a single time point [70,71]. Therefore, we sought to use a bioinformatic approach to quantify the degree of circadian rhythm disruption in the lung caused by acute SD. Principal component analysis of the lung transcriptome allowed us to assess the circadian dysfunction in the lung. The principal directions of a group of 10 circadian transcripts from our ZT transcriptomic dataset (Fig. 2a) were used to project all lung samples onto a 3D space and a spline fitted to represent the expected circadian time and behaviour of the lung (Fig. 2f). Any deviation from this spline would represent an abnormal circadian landscape, and indeed, this is what we found. In contrast to the control samples (black crosses), which fell onto the spline in the expected location, the SD samples (red crosses) were displaced, demonstrating that SD disrupted circadian networks in the lung (Fig. 2f). To quantify the impact on the circadian transcriptome, we used a Support Vector Machine approach to locate the plane that maximally separated the control and SD samples. As can be seen in figure 2g, the optimal plane allowed a clear and significant separation between the SD and control groups (Wilcoxon rank sum test $p = 0.0022$; Fig. 2g). Overall, these data demonstrate that acute SD alters circadian regulation in the lung, and this disruption could contribute towards the increased susceptibility to respiratory viral infection.

Host factors implicated in SARS-CoV-2 infection are differentially expressed in the mouse lung following sleep deprivation

Our data shows that acute SD modifies the transcriptional landscape of the lung in two keys ways to promote infection by respiratory viruses, Firstly, by suppressing the innate and adaptive immune responses, and secondly by disrupting the normal circadian regulatory landscape and physiology of the lung. Three independent studies by Daniloski *et al.* [56], Zhu *et al.* [58], and Wei *et al.* [57] conducted genome-wide CRISPR loss-of-function screens to identify genes regulating SARS-CoV-2 infection. Therefore, we used these data to examine whether SD changes the expression of host factors required by SARS-CoV-2. Daniloski *et al.,* using human alveolar epithelial cells, identified 1,200 potentially relevant genes for SARS-CoV-2 replication and investigated the 50 most highly enriched [56]. Of the 50, 10 were dysregulated following SD (Fig. 3a and d - ACTR2, ACTR3, ATL1, ATP6AP1, ATP6V0B, ATP6V0D1, PIK3C3, SFN, SPEN and WDR81 and Supplementary Table 4), of which 8 could be assigned a putative function in SARS-CoV-2 replication (Fig. 3g). For example, members of the vacuolar-ATPase proton pump, (ATP6V0B, ATP6AP1, and ATP6V0D1), implicated in activation of the SARS-CoV-2 spike protein that is required for viral entry, and ACTR2 and ACTR3, part of the ARP2/3 complex, which functions in endosomal trafficking pathways. Zhu *et al.* identified 32 genes with a potential role in viral entry [58], of which 8 were SD-differential genes (Fig. 3b,d and Supplementary Table 4); four each being up- (NPC1, NPC2, CCDC93, WDR81) and downregulated (COMMD8, COMMD10, ACTR2, ACTR3). All 8 genes play a role in endosomal entry, endolysosomal fusion, or endosome recycling (Fig. 3g). Cross-referencing our SD-differential genes to the 50 most enriched host factors identified by Wei *et al.* [57] revealed an intersection of 11 genes (Fig. 3c and Supplementary Table 4), 8 of which were upregulated and associated primarily with transcriptional regulation (DPF2, JMJD6, RAD54L2, CREBBP, RYBP, ELOA, KMT2D, SIK1 – Fig. 3g). The effect of SD on the individual transcripts that encode for these putative SARS-CoV-2 host factors across all three studies is illustrated in figure 3d. Taken together therefore, acute SD clearly amplifies many host factors and processes that influence multiple steps in the SARS-CoV-2 life cycle.

We next explored if SD-differential genes encode host proteins known to physically interact with SARS-CoV-2 encoded proteins. Gordon *et al.* interrogated human host factors that interact with 26 of the 29 SARS-CoV-2 proteins [55]. The authors identified 332 high confidence human-virus protein-protein interactions, of which 87 overlapped with our SD-differential genes (Fig. 3e,f and Supplementary Table 4). Interestingly, at least 40 of the overlapping genes have a putative function in viral replication, such as RNA processing, ER protein quality control, or intracellular trafficking (Fig. 3g). Furthermore, 18 of the overlapping host factors are involved in mitochondrial processes, ubiquitination, or immune regulation, that may function in SARS-CoV-2 immune evasion (Fig. 3g). Alongside, regulators of signalling pathways, coagulation, and epigenetic modifiers represent some of the other dysregulated classes of interactors that likely impact SARS-CoV-2 infection. Overall, these findings demonstrate that SD causes the differential expression of several host factors that interact with, and are implicated in, SARS-CoV-2 infection that may potentiate virus replication.

The effect of sleep deprivation on SARS-CoV-2 life cycle genes.

When taken together, our data suggest that acute SD impacts many host processes important for the viral life cycle. Using SARS-CoV-2 as an exemplar, we propose a mechanistic pathway, synthesised from the data presented above, by which the SD-differential genes facilitate viral entry, replication, and trafficking (Fig. 4). The extracellular transmembrane protease serine 4 (*Tmprss4*), the protease *Furin*, and *Atp6v0b, Atp6ap1*, and *Atp6v0d1* (members of the vacuolar-ATPase proton pump) all contribute towards spike protein activation and cleavage [72,73], and were differentially expressed following SD, suggesting an increase in virus entry. Following intracellular capsid uncoating the viral RNA is replicated within double membrane vesicles, translated by host ribosomes, and new virus particles assembled and trafficked via the Golgi/ER pathway for release by exocytosis. All these pathways were dysregulated by SD, including transcriptional modulation, endolysosomal fusion, endosome recycling (Fig. 4).

Thirteen genes implicated in intracellular cholesterol trafficking (*Tmem97, Syt7, Npc1, Npc2, Osbpl2, Serac1, Nus1, Vps4a, Anxa2, Lrp6, Atp6ap1, Pik3c3*, and *Wdr81*) were differentially expressed following SD, in line with previous findings showing SD driven disruption of cholesterol metabolism [74]. This was of interest to us, as three of the four cross-referenced SARS-CoV-2 host factor studies (Fig. 3) identified disrupted cholesterol homeostasis as a risk factor for infection. Plasma membrane cholesterol is required for SARS-CoV-2 fusion and cell entry [75], a pathway common to most enveloped viruses. Furthermore, statins have been found to reduce recovery time and decrease the risk for COVID-19 morbidity and mortality [76,77]. How cholesterol impacts SARS-CoV-2 pathogenesis is currently unclear; however, lipid raft disruption, modification of membrane biophysics, alteration of viral stability and maturation, and immune dysfunction have all been suggested as potential mechanisms [78–80].

Finally, SD alters post-translational protein modification that regulates multiple aspects of SARS-CoV-2 replication. For example, the viral nucleocapsid protein is phosphorylated by SRPK1, GSK-3α, and CSNK1 [81] and genes encoding all three kinases were differentially expressed in the lung after SD. Palmitoylation of the Spike envelope glycoprotein is necessary for infectivity. Knockdown of ZDHHC5, a palmitoyltransferase, resulted in spike protein depalmitoylation and compromised membrane fusion and viral entry [82], and SD resulted in increased *Zdhhc5* transcripts in the lung. Overall, these findings suggest that SD could promote SARS-CoV-2 replication by dysregulating many genes involved in its life cycle.

The effect of sleep deprivation on the anti-SARS-CoV-2 immune response and viral immune evasion

Alongside the impact on viral replication, our data shows that SD can suppress immune associated genes allowing viral persistence. Analysis of the SD lung transcriptome shows altered regulation of several components of the immune system (Fig. 5). The regulators of interferon production, RNF41 and TBKBP1, are targeted by SARS-CoV-2 proteins [55] and their genes were differentially expressed following SD. Furthermore, SD caused the differential expression of the E3 ubiquitin ligases *Mib1* and *Trim59*, which induce and repress NF-κB, respectively [83,84], alongside the NF-κB repressor, *Tle1*. These proteins have been shown to associate with SARS-CoV-2 proteins, suggesting that infection interferes with the NF-κB pathway as an immune evasion strategy. Accumulating evidence suggests that SARS-CoV-2 exploits the host ubiquitination machinery to evade the innate immune response [85,86], and intriguingly, six SD differential genes (*Mib1, Rnf41, Usp54, Cul2*, Trim59, Usp13) functionally implicated in ubiquitination, encode proteins that interact with SARS-CoV-2 proteins [55]. Severe

COVID-19 is sometimes associated with syncytia in the lung; multinucleated single cells formed by the fusion of SARS-CoV-2 infected cells to allow viral genome transfer without activating the immune system [87]. Recently, ANO6 has been found to regulate syncytia formation [88], and interestingly, we found that *Ano6* was upregulated following SD. Finally, the manipulation of multiple immune-linked mitochondrial functions is another approach by which respiratory viruses including coronaviruses evade the host immune system [89], and notably we found five SD differential mitochondrial host genes (*Dnajc19, Atp1b1, Dnajc11, Mrps25*, and *Timm29*) which are known to engage in SARS-CoV-2 protein-protein interactions [55]. Taken together therefore, this highlights how acute SD may specifically promote viral immune evasion via multiple complementary pathways.

In conclusion, this study shows that SD alters the transcriptomic landscape in the mouse lung in a manner that could explain the increased risk of respiratory viral infections, as well as severe COVID-19, associated with SCRD and shift work. Suppression of the immune response and promotion of SARS-CoV-2 replication and immune evasion are among the most relevant pathways deregulated by SD. Furthermore, we found a widespread disruption of circadian rhythmicity in the lung following sleep deprivation, which could precipitate and/or exacerbate the negative consequences of SCRD.

Limitations of Study

One limitation of this study is that it only assessed the effect of acute sleep deprivation, not chronic, which would also be very informative. Another limitation of this study was that an *in vivo* challenge experiment was not undertaken. The hypotheses proposed in this study require validation by challenging mice with SARS-CoV-2 after SD; indeed, this would be an important follow-up study. However, these findings help explain why SCRD is associated with severe COVID-19 and could guide future efforts towards understanding the mechanisms underlying SARS-CoV-2 pathogenesis. Importantly, our observations are applicable to a wide range of respiratory viruses and may inform avenues to develop new therapeutic efforts.

ACKNOWLEDGEMENTS

This work was supported by the following sources of funding: BB/N01992X/1 David Phillips fellowship from the BBSRC to AJ, and Oxford-Elysium Cellular Health Fellowship to LT. JAM is funded by a Wellcome Investigator Award 200838/Z/16/Z, UK Medical Research Council (MRC) project grant MR/R022011/1 and Chinese Academy of Medical Sciences (CAMS) Innovation Fund for Medical Science (CIFMS), China (grant number: 2018-I2M-2-002). LU was funded by UK Medical Research Council Doctoral Training Partnership (MR/N014294/1). MV is supported by a grant from Cancer Research UK (C53720/A29468 to RD).

AUTHOR CONTRIBUTIONS

LT, FVL, AA, HS and AJ conducted the experiments. SDP maintained the animals used in this study. LT, FVL, LU, MV and RD analysed data. AJ and SV supervised the study. LT, FVL, JAM and AJ co-wrote and edited the manuscript, with input from all authors.

DECLARATION OF INTERESTS

AJ and SV are cofounders of Circadian Therapeutics Ltd. and hold shares in the company. The following authors hold the current positions: HS is employed by Charles River Associates, FvL by Boston Consulting Group, LU by AstraZeneca and AA by NeuroBio. All other authors declare no competing interests.

INCLUSION AND DIVERSITY

One or more of the authors of this paper self-identifies as an underrepresented ethnic minority in their field of research or within their geographical location. One or more of the authors of this paper self-identifies as a gender minority in their field of research.

FIGURE LEGENDS

Appear below alongside the figures.

STAR METHODS

Resource Availability

Lead contact: Further information and requests for resources and reagents should be directed to and will be fulfilled by the lead contact, Aarti Jagannath (aarti.jagannath@ndcn.ox.ac.uk)

Materials availability: This study did not generate new unique reagents

Data and code availability: All RNA-Seq data have been deposited on NCBI SRA and will be publicly available as of the date of publication. Accession numbers (Bioproject PRJNA914246) are also listed in the key resources table. No original code was used in this study. Any additional information required to reanalyse the data reported in this paper is available from the lead contact upon request.

Experimental Model and Subject Details

Animals

All studies were conducted using male C57BL/6 mice over 8 weeks of age and, unless otherwise indicated, animals were group housed with ad libitum access to food and water under a 12:12 hour light/dark cycle (100 lux from white LED lamps). All animal procedures were conducted in accordance with the UK Home Office regulations (Guidance on the Operation of Animals (Scientific Procedures Act) 1986) and the University of Oxford's Policy on the Use of Animals in Scientific research, following the principles of the 3Rs. For circadian time course analysis, lung tissue was collected at zeitgeber time (ZT)2, ZT8, ZT14, and ZT20. The premise of this study was that COVID-19 infection outcomes are worse in shift-workers. Sleep deprivation (SD) is a core feature of shift work, and the effects of acute SD on both brain and peripheral transcriptomes in mice has been shown to replicate the changes seen in humans shift work-like paradigms, where humans are more chronically sleep-deprived [90,91]. Thus, we sought to profile the effects of acute SD on the lung transcriptome. For the SD experiments, animals were kept awake for 6 hours between ZT0 and ZT6 by providing novel objects to elicit exploratory behaviour, as previously described [92]. The animals were then sacrificed, and lung tissue collected. Control animals were allowed to sleep ad libitum between ZT0 and ZT6. Recovery sleep (RS) animals were sleep deprived for 6 hours, as detailed above, and then allowed to sleep ad libitum for 3 hours before being sacrificed and lung tissue collected.

Method Details

RNA extraction and RNA sequencing library preparation

Total RNA from lung tissue samples was extracted using TRIzol and the RNeasy Mini Kit (Qiagen). Lung tissue was mechanically disrupted in 700 µl of TRIzol and 140 µl of chloroform was added and the sample thoroughly mixed. Following a 3 min incubation at RT, the sample was then centrifuged for 15 min at 15,000 xg, 4°C. The clear top layer was then carefully collected, mixed with an equal volume of 70% ethanol and RNA extracted using the RNeasy Mini Kit, with on-column DNase digestion, following the manufacturer's instructions. RNA was eluted in water and RNA concentration and quality were measured using a TapeStation system (Agilent) with the High Sensitivity RNA ScreenTape assay. mRNA purification and cDNA synthesis for the sequencing library were performed according to the Illumina Stranded mRNA Prep protocol (20040534) using the following index kit: IDT for Illumina RNA UD Indexes Set A, Ligation (20040553). Quality and concentration of the final libraries were checked with the KAPA Library Quantification Kit (Roche Diagnostics) in a StepOnePlus thermal cycler (Applied Biosystems) according to manufacturer's instructions. All cDNA libraries were sequenced using a paired-end strategy (read length 150 bp) on an Illumina NovaSeq platform.

Lung protein extraction

Lung tissue was placed into an appropriate volume of tissue lysis buffer (500 µl/10 mg tissue – 100 mM Tris, 150 mM NaCl, 1 mM EGTA, 1 mM EDTA, 1% Triton-X100, 0.5% Sodium deoxycholate, pH 7.4) supplemented with protease inhibitors (Roche, UK), and then lysed in a glass dounce homogeniser (Sigma, UK). The samples were incubated on ice for 10 min, vortexed, and then placed back on ice for a further 10 min before being centrifuged for 20 min at 13,000 xg, 4°C. The protein concentration of the debris free supernatant was determined using the Pierce™ BCA Protein Assay Kit (Thermo Fisher scientific, Loughborough, UK) following the manufacturer's protocol. The samples were then diluted to 1 mg/mL using reagent diluent (RD – PBS + 1% BSA), aliquoted and then stored at -80°C.

ELISA

The concentration of murine CCL5, TNF-α, IL-6 and IFN-γ in total lung homogenate was determined using DuoSet® sandwich ELISA assays (R & D systems). To begin, a 96 well MAXISORP plate (Thermo Scientific) was coated with capture antibody, diluted to the desired working concentration in PBS, overnight at RT. The plate was then washed by completely filling each well with wash buffer (PBS containing 0.05% tween), followed by aspiration, four times. Plates were then blocked by the addition of 300 µl of RD per well and incubation for 1 hour at RT. The plates were then washed four times with wash buffer and 100 µl of sample or protein standard diluted in reagent diluent was added per well and the plate incubated for 2 hours at RT. Following another wash step, detection antibody diluted in reagent diluent was added to each well and the plate incubated for 2 hours at RT. The plates were subjected to another wash step and streptavidin-HRP added to each well and the plate incubated for 20 min at RT. The plates then had one final round of washing after which 55 µl of 1-Step Ultra TMB-ELISA solution was added to each well and the plates incubated for 15 min at RT in the dark. Finally, 55 µl of 2N H_2SO_4 was added to each well to stop the HRP reaction and the

absorbance at 450 nm for each well was determined using a FLUOstar OMEGA plate reader. These values were corrected by subtracting absorbance at 570 nm. The amount of each analyte was then determined by interpolation from the protein standard curve, taking into account the dilution factor of each sample.

qRT-PCR

Total RNA was extracted from mouse lung tissue as detailed above and cDNA was synthesized using the qScript cDNA Synthesis Kit (Quantabio). mRNA was quantified using the QuantiFast SYBR Green PCR Kit (Qiagen) in a StepOnePlus thermal cycler. Cycling conditions were 95 °C for 5 min, and 40 cycles of 95 °C for 10 s, 60 °C for 30 s, 72 °C for 12 s. The cycle thresholds for each gene were normalized using ActB, Gapdh, and Rn18s as housekeeping genes following the $2^{-\Delta Ct}$ method. The primers used qRT-PCR analysis are listed in Supplementary Table 7.

Processing of RNA sequencing data

Raw RNA-Seq data processing (quality control, trimming, mapping to the genome, and read counting) was performed using tools embedded in Galaxy (v21.05) [93]. The fastqsanger files containing the raw sequencing data were uploaded to the public Galaxy server at usegalaxy.org. FastQC (v0.11.8) (https://www.bioinformatics.babraham.ac.uk/projects/fastqc/) was used for quality control of sequencing data. For quality and adapter trimming, Trim Galore! (v0.6.3) (https://www.bioinformatics.babraham.ac.uk/projects/trim_galore/) was employed to remove low-quality bases, short reads, and Illumina adapters. Nextera transposase was specified as the adapter sequence to be trimmed and Trim Galore! was instructed to remove 1 bp from the 5' end of both read 1 and 2. FastQC was rerun to assess the quality improvement. High quality reads were then mapped to the Mus musculus (mm10) reference genome using HISAT2 (v2.1.0) [94], specifying the strand information as reverse. featureCounts (v2.0.1) [95] was run to quantify the number of reads mapped to each gene. The featureCounts built-in mm10 gene annotation file was selected and under paired-end reads options, the option to count fragments instead of reads was enabled. The generated counts files were converted to CSV and downloaded for downstream differential gene expression analysis in R. MultiQC (v1.9) [96] was used to aggregate FastQC, HISAT2, and featureCounts results.

Differential gene expression analysis

To identify differentially expressed genes in the SD and times series (ZT) datasets, the DESeq2 package (v1.32.0) [97] was used in R (v4.1.0). DESeq2 corrects for multiple testing using the Benjamini-Hochberg (BH) method, and only genes with a BH adjusted p value < 0.05 were considered statistically significant. Heatmaps were drawn using the pheatmap function from the pheatmap package (v1.0.12). Volcano plots were generated using the ggplot2 package (v.3.3.5).

To detect periodicity in the time series (ZT) data, the MetaCycle R package (v1.2.0) was used [98]. The meta2d function was run using the MetaCycle web application (MetaCycleApp) based on the shiny package (v1.6.0). The following parameters were specified: minper = 24, maxper = 24, ARSdefaultPER = 24, cycMethod = JTK, combinePvalue = fisher. Any gene with a

corrected q value of < 0.05 was considered significantly rhythmic. The MetaCycleApp was downloaded from https://github.com/gangwug/MetaCycleApp.

Functional enrichment analysis

Functional enrichment analysis of SD-associated genes and cycling genes was conducted using the clusterProfiler R package (v4.0.0) [99]. GO BP and KEGG analysis was performed using the enrichGO function, with org.Mm.eg.db (v3.13.0) as the Mus musculus genome annotation (GO BP parameters - pvalueCutoff = 0.01, qvalueCutoff = 0.05, pAdjustMethod = Benjamini–Hochberg correction and KEGG paramerters - pvalueCutoff = 0.05). Enriched KEGG terms were visualised using a custom R script. The network interaction between overrepresented GO BP pathways was visualized using the ClueGO application (v2.5.8) [100] and its plugin CluePedia (v1.5.8) [101] within the desktop version of the Cytoscape software (v3.8.2) [102]. The yFiles Organic Layout from the yFiles Layout Algorithms application (v1.1.1) [103] was used to specify the design. Transcription factor enrichment analysis was performed using Enrichr [104] and the ChEA3 database. The combined score was used to assess significance of enrichment. The SARS-CoV-2 gene set enrichment analysis was performed using Enrichr and the COVID-19 Drug and Gene Set Library.

Principal component analysis projection of circadian and SD transcript expression

To assess the circadian behaviour of the mouse lung we used principal component analysis (PCA). We first reduced the transcriptomic datasets to 10 circadian features, i.e., transcripts known to be highly rhythmic across murine organ systems (Arntl, Per2, Per3, Tef, Hlf, Dbp, Nr1d1, Nr1d2, Npas2, and Dtx4) [105]. The resultant transcript x sample matrices were log-transformed and then Z-score normalised column-wise to prepare the data for dimensionality reduction. Singular value decomposition was applied to the 16 samples collected at times ZT2, ZT8, ZT14, and ZT20 to obtain the principal directions (using the svd function in MATLAB v2020b). All lung samples (time course and SD) were then projected onto the 3D principal component space generated from the first three principal directions of the time course samples. The time point means of the projected time course samples were estimated by fitting Gaussian distributions. A shape-preserving cubic spline was fitted through the estimated means of the projected time course samples to approximate the expected circadian behaviour of the mouse lung (using the csape function in MATLAB). The Support Vector Machine approach (package gensvm v.0.1.5 in R v.4.1.1) with the linear kernel was then used to find the equation of the plane which optimally separated the control and SD lung samples in the 3D principal component space, and then all samples were projected onto the normal of the plane. A Wilcoxon's rank sum test was carried out in MATLAB (ranksum function) for the projections on the normal to determine whether the null hypothesis that the control and SD samples belonged to the same population (same median) could be rejected.

Quantification and Statistical analysis

All data are expressed as mean + or ± SEM, and n represents the number of independent animals or replicates per group, as detailed in each figure legend. For comparisons between two groups only, a one-tailed unpaired Student's t-test was used. Statistical significance of gene set overlaps was assessed by two-tailed Fisher's exact test, assuming 21,647 total genes in the lung transcriptome as determined by the RNA-Seq data from SD and time series

analysis in this study. Correlation between the qRT-PCR and RNA-Seq expression data was examined using two-tailed Pearson correlation analysis. Statistical testing was performed in R, MATLAB, and GraphPad Prism 9 (v9.1.2).

Key Resources Table

KEY RESOURCES TABLE

REAGENT or RESOURCE	SOURCE	IDENTIFIER
Critical Commercial Assays		
Illumina TruSeq Stranded Total RNA library prep gold kit	Illumina	Cat#20020598
NextSeq 550 and a Nextseq 500/500 v2.5 75 cycle kit	Illumina	Cat#20024906
KAPA library quantification kit	Roche	Cat#07960140001
BCA protein assay kit	Life Technologies	Cat#23225
Mouse TNF-alpha DuoSet ELISA	R&D Systems	DY410-05
Mouse IL-6 DuoSet ELISA	R&D Systems	DY406
Mouse IFN-gamma DuoSet ELISA	R&D Systems	DY485
Mouse CCL5/RANTES DuoSet ELISA	R&D Systems	DY478
Deposited Data		
Chea3 transcription factor database	https://maayanlab.cloud/Enrichr/	
COVID-19 Drug and Gene Set Library	https://maayanlab.cloud/Enrichr/	
Experimental Models: Organisms/Strains		
Mouse: C56Bl6/J	Envigo	
Oligonucleotides		
Primer sequences in Supplementary Table 7		
Software and Algorithms		
Clocklab	Actimetrics	https://www.actimetrics.com/products/clocklab/
Prism 8	GraphPad	https://www.graphpad.com/

HISAT2	(Kim et al., 2019)	http://daehwankimlab.github.io/hisat2/about/
FeatureCounts	(Liao et al., 2014)	http://subread.sourceforge.net/
DeSeq2	(Love et al., 2014)	https://bioconductor.org/packages/release/bioc/html/DESeq2.html
Fastq files	NCBI SRA	Accession number PRJNA914246

REFERENCES

1. Jin, X., Ren, J., Li, R., Gao, Y., Zhang, H., Li, J., Zhang, J., Wang, X., and Wang, G. (2021). Global burden of upper respiratory infections in 204 countries and territories, from 1990 to 2019. EClinicalMedicine *37*. 10.1016/J.ECLINM.2021.100986/ATTACHMENT/F7CE630F-8826-46F7-AB34-DC964B584FC2/MMC2.PDF.
2. Troeger, C., Blacker, B., Khalil, I.A., Rao, P.C., Cao, J., Zimsen, S.R.M., Albertson, S.B., Deshpande, A., Farag, T., Abebe, Z., et al. (2018). Estimates of the global, regional, and national morbidity, mortality, and aetiologies of lower respiratory infections in 195 countries, 1990–2016: a systematic analysis for the Global Burden of Disease Study 2016. Lancet Infect Dis *18*, 1191–1210. 10.1016/S1473-3099(18)30310-4/ATTACHMENT/2D345E43-7661-476D-89A4-0EDC7D913C4C/MMC1.PDF.
3. Molinari, N.A.M., Ortega-Sanchez, I.R., Messonnier, M.L., Thompson, W.W., Wortley, P.M., Weintraub, E., and Bridges, C.B. (2007). The annual impact of seasonal influenza in the US: measuring disease burden and costs. Vaccine *25*, 5086–5096. 10.1016/J.VACCINE.2007.03.046.
4. Fendrick, A.M., Monto, A.S., Nightengale, B., and Sarnes, M. (2003). The economic burden of non-influenza-related viral respiratory tract infection in the United States. Arch Intern Med *163*, 487–494. 10.1001/ARCHINTE.163.4.487.
5. Zhu, N., Zhang, D., Wang, W., Li, X., Yang, B., Song, J., Zhao, X., Huang, B., Shi, W., Lu, R., et al. (2020). A Novel Coronavirus from Patients with Pneumonia in China, 2019. New England Journal of Medicine *382*, 727–733. 10.1056/NEJMOA2001017/SUPPL_FILE/NEJMOA2001017_DISCLOSURES.PDF.
6. Ehlers, A., Xie, W., Agapov, E., Brown, S., Steinberg, D., Tidwell, R., Sajol, G., Schutz, R., Weaver, R., Yu, H., et al. (2018). BMAL1 LINKS THE CIRCADIAN CLOCK TO VIRAL AIRWAY PATHOLOGY AND ASTHMA PHENOTYPES. Mucosal Immunol *11*, 97. 10.1038/MI.2017.24.
7. Brown, R., Pang, G., Husband, A.J., and King, M.G. (1989). Suppression of immunity to influenza virus infection in the respiratory tract following sleep disturbance. Reg Immunol *2*, 321–325.
8. Prather, A.A., and Leung, C.W. (2016). Association of Insufficient Sleep With Respiratory Infection Among Adults in the United States. JAMA Intern Med *176*, 850. 10.1001/JAMAINTERNMED.2016.0787.
9. Prather, A.A., Janicki-Deverts, D., Hall, M.H., and Cohen, S. (2015). Behaviorally assessed sleep and susceptibility to the common cold. Sleep *38*. 10.5665/sleep.4968.
10. Robinson, C.H., Albury, C., McCartney, D., Fletcher, B., Roberts, N., Jury, I., and Lee, J. (2021). The relationship between duration and quality of sleep and upper respiratory tract infections: a systematic review. Fam Pract *38*, 802–810. 10.1093/FAMPRA/CMAB033.
11. Ragnoli, B., Pochetti, P., Pignatti, P., Barbieri, M., Mondini, L., Ruggero, L., Trotta, L., Montuschi, P., and Malerba, M. (2022). Sleep Deprivation, Immune Suppression and

SARS-CoV-2 Infection. Int J Environ Res Public Health *19*. 10.3390/IJERPH19020904.

12. Maidstone, R., Anderson, S.G., Ray, D.W., Rutter, M.K., Durrington, H.J., and Blaikley, J.F. (2021). Shift work is associated with positive COVID-19 status in hospitalised patients. Thorax *76*, 601–606. 10.1136/THORAXJNL-2020-216651.
13. Lim, R.K., Wambier, C.G., and Goren, A. (2020). Are night shift workers at an increased risk for COVID-19? Med Hypotheses *144*. 10.1016/j.mehy.2020.110147.
14. Fatima, Y., Bucks, R.S., Mamun, A.A., Skinner, I., Rosenzweig, I., Leschziner, G., and Skinner, T.C. (2021). Shift work is associated with increased risk of COVID-19: Findings from the UK Biobank cohort. J Sleep Res *30*. 10.1111/JSR.13326.
15. Rowlands, A. v., Gillies, C., Chudasama, Y., Davies, M.J., Islam, N., Kloecker, D.E., Lawson, C., Pareek, M., Razieh, C., Zaccardi, F., et al. (2021). Association of working shifts, inside and outside of healthcare, with severe COVID−19: an observational study. BMC Public Health *21*, 1–7. 10.1186/S12889-021-10839-0/FIGURES/2.
16. Kim, H., Hegde, S., Lafiura, C., Raghavan, M., Luong, E., Cheng, S., Rebholz, C.M., and Seidelmann, S.B. (2021). COVID-19 illness in relation to sleep and burnout. BMJ Nutr Prev Health *4*, 132. 10.1136/BMJNPH-2021-000228.
17. Hastings, M.H., Maywood, E.S., and Brancaccio, M. (2018). Generation of circadian rhythms in the suprachiasmatic nucleus. Nat Rev Neurosci *19*, 453–469. 10.1038/s41583-018-0026-z.
18. Golombek, D.A., and Rosenstein, R.E. (2010). Physiology of Circadian Entrainment. Physiol Rev *90*, 1063–1102. 10.1152/physrev.00009.2009.
19. Rijo-Ferreira, F., and Takahashi, J.S. (2019). Genomics of circadian rhythms in health and disease. Genome Medicine 2019 11:1 *11*, 1–16. 10.1186/S13073-019-0704-0.
20. Labrecque, N., and Cermakian, N. (2015). Circadian clocks in the immune system. J Biol Rhythms *30*, 277–290. 10.1177/0748730415577723.
21. Scheiermann, C., Kunisaki, Y., and Frenette, P.S. (2013). Circadian control of the immune system. Nat Rev Immunol *13*, 190. 10.1038/NRI3386.
22. Cermakian, N., Stegeman, S.K., Tekade, K., and Labrecque, N. (2021). Circadian rhythms in adaptive immunity and vaccination. Semin Immunopathol, 1–15. 10.1007/S00281-021-00903-7/TABLES/1.
23. Wang, W., Balfe, P., Eyre, D.W., Lumley, S.F., O'Donnell, D., Warren, F., Crook, D.W., Jeffery, K., Matthews, P.C., Klerman, E.B., et al. (2022). Time of Day of Vaccination Affects SARS-CoV-2 Antibody Responses in an Observational Study of Health Care Workers. J Biol Rhythms *37*, 124. 10.1177/07487304211059315.
24. Long, J.E., Drayson, M.T., Taylor, A.E., Toellner, K.M., Lord, J.M., and Phillips, A.C. (2016). Morning vaccination enhances antibody response over afternoon vaccination: A cluster-randomised trial. Vaccine *34*, 2679–2685. 10.1016/J.VACCINE.2016.04.032.
25. Phillips, A.C., Gallagher, S., Carroll, D., and Drayson, M. (2008). Preliminary evidence that morning vaccination is associated with an enhanced antibody response in men. Psychophysiology *45*, 663–666. 10.1111/J.1469-8986.2008.00662.X.
26. Sengupta, S., Tang, S.Y., Devine, J.C., Anderson, S.T., Nayak, S., Zhang, S.L., Valenzuela, A., Fisher, D.G., Grant, G.R., López, C.B., et al. (2019). Circadian control of lung inflammation in influenza infection. Nature Communications 2019 10:1 *10*, 1–13. 10.1038/s41467-019-11400-9.
27. Edgar, R.S., Stangherlin, A., Nagy, A.D., Nicoll, M.P., Efstathiou, S., O'Neill, J.S., and Reddy, A.B. (2016). Cell autonomous regulation of herpes and influenza virus infection by the circadian clock. Proc Natl Acad Sci U S A *113*, 10085–10090. 10.1073/PNAS.1601895113/-/DCSUPPLEMENTAL.
28. Matsuzawa, T., Nakamura, Y., Ogawa, Y., Ishimaru, K., Goshima, F., Shimada, S., Nakao, A., and Kawamura, T. (2018). Differential Day-Night Outcome to HSV-2 Cutaneous Infection. Journal of Investigative Dermatology *138*, 233–236. 10.1016/J.JID.2017.07.838.

29. Gagnidze, K., Hajdarovic, K.H., Moskalenko, M., Karatsoreos, I.N., McEwen, B.S., and Bulloch, K. (2016). Nuclear receptor REV-ERBα mediates circadian sensitivity to mortality in murine vesicular stomatitis virus-induced encephalitis. Proc Natl Acad Sci U S A *113*, 5730–5735. 10.1073/PNAS.1520489113.
30. Castanon-Cervantes, O., Wu, M., Ehlen, J.C., Paul, K., Gamble, K.L., Johnson, R.L., Besing, R.C., Menaker, M., Gewirtz, A.T., and Davidson, A.J. (2010). Dysregulation of Inflammatory Responses by Chronic Circadian Disruption. The Journal of Immunology *185*, 5796–5805. 10.4049/JIMMUNOL.1001026.
31. Scheiermann, C., Gibbs, J., Ince, L., and Loudon, A. (2018). Clocking in to immunity. Nature Reviews Immunology 2018 18:7 *18*, 423–437. 10.1038/s41577-018-0008-4.
32. Zhuang, X., Magri, A., Hill, M., Lai, A.G., Kumar, A., Rambhatla, S.B., Donald, C.L., Lopez-Clavijo, A.F., Rudge, S., Pinnick, K., et al. (2019). The circadian clock components BMAL1 and REV-ERBα regulate flavivirus replication. Nat Commun *10*. 10.1038/s41467-019-08299-7.
33. Majumdar, T., Dhar, J., Patel, S., Kondratov, R., and Barik, S. (2017). Circadian transcription factor BMAL1 regulates innate immunity against select RNA viruses. Innate Immun *23*, 147–154. 10.1177/1753425916681075.
34. Zhuang, X., Forde, D., Tsukuda, S., D'Arienzo, V., Mailly, L., Harris, J.M., Wing, P.A.C., Borrmann, H., Schilling, M., Magri, A., et al. (2021). Circadian control of hepatitis B virus replication. Nat Commun *12*. 10.1038/s41467-021-21821-0.
35. Sundar, I.K., Ahmad, T., Yao, H., Hwang, J.W., Gerloff, J., Lawrence, B.P., Sellix, M.T., and Rahman, I. (2015). Influenza A virus-dependent remodeling of pulmonary clock function in a mouse model of COPD. Sci Rep *4*. 10.1038/SREP09927.
36. Borrmann, H., McKeating, J.A., and Zhuang, X. (2021). The Circadian Clock and Viral Infections. J Biol Rhythms *36*, 9. 10.1177/0748730420967768.
37. Scammell, T.E., Arrigoni, E., and Lipton, J.O. (2017). Neural Circuitry of Wakefulness and Sleep. Neuron *93*, 747–765. 10.1016/j.neuron.2017.01.014.
38. Borbély, A.A., Daan, S., Wirz-Justice, A., and Deboer, T. (2016). The two-process model of sleep regulation: a reappraisal. J Sleep Res *25*, 131–143. 10.1111/JSR.12371.
39. Irwin, M., McClintick, J., Costlow, C., Fortner, M., White, J., and Gillin, J.C. (1996). Partial night sleep deprivation reduces natural killer and cellular immune responses in humans. FASEB J *10*, 643–653. 10.1096/FASEBJ.10.5.8621064.
40. Irwin, M., Thompson, J., Miller, C., Gillin, J.C., and Ziegler, M. (1999). Effects of sleep and sleep deprivation on catecholamine and interleukin-2 levels in humans: clinical implications. J Clin Endocrinol Metab *84*, 1979–1985. 10.1210/JCEM.84.6.5788.
41. Redwine, L., Hauger, R.L., Gillin, J.C., and Irwin, M. (2000). Effects of sleep and sleep deprivation on interleukin-6, growth hormone, cortisol, and melatonin levels in humans. J Clin Endocrinol Metab *85*, 3597–3603. 10.1210/JCEM.85.10.6871.
42. Wright, K.P., Drake, A.L., Frey, D.J., Fleshner, M., Desouza, C.A., Gronfier, C., and Czeisler, C.A. (2015). Influence of Sleep Deprivation and Circadian Misalignment on Cortisol, Inflammatory Markers, and Cytokine Balance. Brain Behav Immun *47*, 24. 10.1016/J.BBI.2015.01.004.
43. Haack, M., Sanchez, E., and Mullington, J.M. (2007). Elevated inflammatory markers in response to prolonged sleep restriction are associated with increased pain experience in healthy volunteers. Sleep *30*, 1145–1152. 10.1093/SLEEP/30.9.1145.
44. Besedovsky, L., Lange, T., and Haack, M. (2019). The Sleep-Immune Crosstalk in Health and Disease. Physiol Rev *99*, 1325. 10.1152/PHYSREV.00010.2018.
45. Archer, S.N., and Oster, H. (2015). How sleep and wakefulness influence circadian rhythmicity: effects of insufficient and mistimed sleep on the animal and human transcriptome. J Sleep Res *24*, 476–493. 10.1111/JSR.12307.
46. Hor, C.N., Yeung, J., Jan, M., Emmenegger, Y., Hubbard, J., Xenarios, I., Naef, F., and Franken, P. (2019). Sleep–wake-driven and circadian contributions to daily rhythms in gene expression and chromatin accessibility in the murine cortex. Proc

Natl Acad Sci U S A *116*, 25773–25783. 10.1073/PNAS.1910590116/-/DCSUPPLEMENTAL.

47. Husse, J., Kiehn, J.T., Barclay, J.L., Naujokat, N., Meyer-Kovac, J., Lehnert, H., and Oster, H. (2017). Tissue-Specific Dissociation of Diurnal Transcriptome Rhythms During Sleep Restriction in Mice. Sleep *40*. 10.1093/SLEEP/ZSX068.
48. Anafi, R.C., Pellegrino, R., Shockley, K.R., Romer, M., Tufik, S., and Pack, A.I. (2013). Sleep is not just for the brain: transcriptional responses to sleep in peripheral tissues. BMC Genomics *14*, 362. 10.1186/1471-2164-14-362.
49. Lu, Y., Liu, B., Ma, J., Yang, S., and Huang, J. (2021). Disruption of Circadian Transcriptome in Lung by Acute Sleep Deprivation. Front Genet *12*, 477. 10.3389/FGENE.2021.664334/BIBTEX.
50. Möller-Levet, C.S., Archer, S.N., Bucca, G., Laing, E.E., Slak, A., Kabiljo, R., Lo, J.C.Y., Santhi, N., von Schantz, M., Smith, C.P., et al. (2013). Effects of insufficient sleep on circadian rhythmicity and expression amplitude of the human blood transcriptome. Proc Natl Acad Sci U S A *110*. 10.1073/PNAS.1217154110.
51. Foo, J.C., Trautmann, N., Sticht, C., Treutlein, J., Frank, J., Streit, F., Witt, S.H., de La Torre, C., von Heydendorff, S.C., Sirignano, L., et al. (2019). Longitudinal transcriptome-wide gene expression analysis of sleep deprivation treatment shows involvement of circadian genes and immune pathways. Translational Psychiatry 2019 9:1 *9*, 1–10. 10.1038/s41398-019-0671-7.
52. Cuesta, M., Boudreau, P., Dubeau-Laramée, G., Cermakian, N., and Boivin, D.B. (2016). Simulated Night Shift Disrupts Circadian Rhythms of Immune Functions in Humans. J Immunol *196*, 2466–2475. 10.4049/JIMMUNOL.1502422.
53. Cohen, S., Doyle, W.J., Alper, C.M., Janicki-Deverts, D., and Turner, R.B. (2009). Sleep Habits and Susceptibility to the Common Cold. Arch Intern Med *169*, 62–67. 10.1001/ARCHINTERNMED.2008.505.
54. Rizza, S., Coppeta, L., Grelli, S., Ferrazza, G., Chiocchi, M., Vanni, G., Bonomo, O.C., Bellia, A., Andreoni, M., Magrini, A., et al. (2021). High body mass index and night shift work are associated with COVID-19 in health care workers. J Endocrinol Invest *44*, 1. 10.1007/S40618-020-01397-0.
55. Gordon, D.E., Jang, G.M., Bouhaddou, M., Xu, J., Obernier, K., White, K.M., O'Meara, M.J., Rezelj, V. v., Guo, J.Z., Swaney, D.L., et al. (2020). A SARS-CoV-2 protein interaction map reveals targets for drug repurposing. Nature *583*. 10.1038/s41586-020-2286-9.
56. Daniloski, Z., Jordan, T.X., Wessels, H.H., Hoagland, D.A., Kasela, S., Legut, M., Maniatis, S., Mimitou, E.P., Lu, L., Geller, E., et al. (2021). Identification of Required Host Factors for SARS-CoV-2 Infection in Human Cells. Cell *184*, 92-105.e16. 10.1016/J.CELL.2020.10.030.
57. Wei, J., Alfajaro, M.M., DeWeirdt, P.C., Hanna, R.E., Lu-Culligan, W.J., Cai, W.L., Strine, M.S., Zhang, S.M., Graziano, V.R., Schmitz, C.O., et al. (2021). Genome-wide CRISPR Screens Reveal Host Factors Critical for SARS-CoV-2 Infection. Cell *184*, 76-91.e13. 10.1016/J.CELL.2020.10.028.
58. Zhu, Y., Feng, F., Hu, G., Wang, Y., Yu, Y., Zhu, Y., Xu, W., Cai, X., Sun, Z., Han, W., et al. (2021). A genome-wide CRISPR screen identifies host factors that regulate SARS-CoV-2 entry. Nature Communications 2021 12:1 *12*, 1–11. 10.1038/s41467-021-21213-4.
59. Reutershan, J., Basit, A., Galkina, E. v., and Ley, K. (2005). Sequential recruitment of neutrophils into lung and bronchoalveolar lavage fluid in LPS-induced acute lung injury. Am J Physiol Lung Cell Mol Physiol *289*, 807–815. 10.1152/AJPLUNG.00477.2004/ASSET/IMAGES/LARGE/ZH50110543590007.JPEG.
60. Chignard, M., and Balloy, V. (2000). Neutrophil recruitment and increased permeability during acute lung injury induced by lipopolysaccharide. Am J Physiol Lung Cell Mol Physiol *279*. 10.1152/AJPLUNG.2000.279.6.L1083/ASSET/IMAGES/LARGE/H51200184008.JPEG.

61. Kuleshov, M. v., Stein, D.J., Clarke, D.J.B., Kropiwnicki, E., Jagodnik, K.M., Bartal, A., Evangelista, J.E., Hom, J., Cheng, M., Bailey, A., et al. (2020). The COVID-19 Drug and Gene Set Library. Patterns *1*. 10.1016/j.patter.2020.100090.
62. Li, S., Ma, F., Yokota, T., Garcia, G., Palermo, A., Wang, Y., Farrell, C., Wang, Y.C., Wu, R., Zhou, Z., et al. (2021). Metabolic reprogramming and epigenetic changes of vital organs in SARS-CoV-2-induced systemic toxicity. JCI Insight *6*. 10.1172/JCI.INSIGHT.145027.
63. Johnson, B.A., Xie, X., Bailey, A.L., Kalveram, B., Lokugamage, K.G., Muruato, A., Zou, J., Zhang, X., Juelich, T., Smith, J.K., et al. (2021). Loss of furin cleavage site attenuates SARS-CoV-2 pathogenesis. Nature 2021 591:7849 *591*, 293–299. 10.1038/s41586-021-03237-4.
64. Khanmohammadi, S., and Rezaei, N. (2021). Role of Toll-like receptors in the pathogenesis of COVID-19. J Med Virol *93*, 2735–2739. 10.1002/JMV.26826.
65. Mabrey, F.L., Morrell, E.D., and Wurfel, M.M. (2021). TLRs in COVID-19: How they drive immunopathology and the rationale for modulation. Innate Immun *27*, 503–513. 10.1177/17534259211051364.
66. Suzuki, A., Sinton, C.M., Greene, R.W., and Yanagisawa, M. (2013). Behavioral and biochemical dissociation of arousal and homeostatic sleep need influenced by prior wakeful experience in mice. Proc Natl Acad Sci U S A *110*, 10288–10293. 10.1073/PNAS.1308295110/SUPPL_FILE/PNAS.201308295SI.PDF.
67. Bellesi, M., Haswell, J.D., de Vivo, L., Marshall, W., Roseboom, P.H., Tononi, G., and Cirelli, C. (2018). Myelin modifications after chronic sleep loss in adolescent mice. Sleep *41*. 10.1093/SLEEP/ZSY034.
68. Mongrain, V., Hernandez, S.A., Pradervand, S., Dorsaz, S., Curie, T., Hagiwara, G., Gip, P., Heller, H.C., and Franken, P. (2010). Separating the contribution of glucocorticoids and wakefulness to the molecular and electrophysiological correlates of sleep homeostasis. Sleep *33*, 1147–1157. 10.1093/SLEEP/33.9.1147.
69. Jagannath, A., Varga, N., Dallmann, R., Rando, G., Gosselin, P., Ebrahimjee, F., Taylor, L., Mosneagu, D., Stefaniak, J., Walsh, S., et al. (2021). Adenosine integrates light and sleep signalling for the regulation of circadian timing in mice. Nature Communications 2021 12:1 *12*, 1–11. 10.1038/s41467-021-22179-z.
70. Naef, F., and Talamanca, L. (2020). How to tell time: advances in decoding circadian phase from omics snapshots. F1000Res *9*. 10.12688/F1000RESEARCH.26759.1.
71. Anafi, R.C., Francey, L.J., Hogenesch, J.B., and Kim, J. (2017). CYCLOPS reveals human transcriptional rhythms in health and disease. Proc Natl Acad Sci U S A *114*, 5312–5317. 10.1073/PNAS.1619320114.
72. Zang, R., Castro, M.F.G., McCune, B.T., Zeng, Q., Rothlauf, P.W., Sonnek, N.M., Liu, Z., Brulois, K.F., Wang, X., Greenberg, H.B., et al. (2020). TMPRSS2 and TMPRSS4 promote SARS-CoV-2 infection of human small intestinal enterocytes. Sci Immunol *5*, 3582. 10.1126/SCIIMMUNOL.ABC3582/SUPPL_FILE/ABC3582_TABLE_S3.XLSX.
73. Tang, T., Bidon, M., Jaimes, J.A., Whittaker, G.R., and Daniel, S. (2020). Coronavirus membrane fusion mechanism offers a potential target for antiviral development. Antiviral Res *178*. 10.1016/J.ANTIVIRAL.2020.104792.
74. Aho, V., Ollila, H.M., Kronholm, E., Bondia-Pons, I., Soininen, P., Kangas, A.J., Hilvo, M., Seppälä, I., Kettunen, J., Oikonen, M., et al. (2016). Prolonged sleep restriction induces changes in pathways involved in cholesterol metabolism and inflammatory responses. Sci Rep *6*. 10.1038/SREP24828.
75. Wang, S., Li, W., Hui, H., Tiwari, S.K., Zhang, Q., Croker, B.A., Rawlings, S., Smith, D., Carlin, A.F., and Rana, T.M. (2020). Cholesterol 25-Hydroxylase inhibits SARS-CoV-2 and other coronaviruses by depleting membrane cholesterol. EMBO J *39*. 10.15252/EMBJ.2020106057.
76. Zhang, X.J., Qin, J.J., Cheng, X., Shen, L., Zhao, Y.C., Yuan, Y., Lei, F., Chen, M.M., Yang, H., Bai, L., et al. (2020). In-Hospital Use of Statins Is Associated with a Reduced Risk of Mortality among Individuals with COVID-19. Cell Metab *32*, 176-187.e4. 10.1016/J.CMET.2020.06.015.

77. Daniels, L.B., Sitapati, A.M., Zhang, J., Zou, J., Bui, Q.M., Ren, J., Longhurst, C.A., Criqui, M.H., and Messer, K. (2020). Relation of Statin Use Prior to Admission to Severity and Recovery Among COVID-19 Inpatients. Am J Cardiol *136*, 149–155. 10.1016/J.AMJCARD.2020.09.012.
78. Tang, Y., Hu, L., Liu, Y., Zhou, B., Qin, X., Ye, J., Shen, M., Wu, Z., and Zhang, P. (2021). Possible mechanisms of cholesterol elevation aggravating COVID-19. Int J Med Sci *18*, 3533. 10.7150/IJMS.62021.
79. Li, X., Zhu, W., Fan, M., Zhang, J., Peng, Y., Huang, F., Wang, N., He, L., Zhang, L., Holmdahl, R., et al. (2021). Dependence of SARS-CoV-2 infection on cholesterol-rich lipid raft and endosomal acidification. Comput Struct Biotechnol J *19*, 1933–1943. 10.1016/J.CSBJ.2021.04.001.
80. Schmidt, N.M., Wing, P.A.C., McKeating, J.A., and Maini, M.K. (2020). Cholesterol-modifying drugs in COVID-19. Oxf Open Immunol *1*. 10.1093/OXFIMM/IQAA001.
81. Yaron, T.M., Heaton, B.E., Levy, T.M., Johnson, J.L., Jordan, T.X., Cohen, B.M., Kerelsky, A., Lin, T.-Y., Liberatore, K.M., Bulaon, D.K., et al. (2020). The FDA-approved drug Alectinib compromises SARS-CoV-2 nucleocapsid phosphorylation and inhibits viral infection in vitro. bioRxiv. 10.1101/2020.08.14.251207.
82. Wu, Z., Zhang, Z., Wang, X., Zhang, J., Ren, C., Li, Y., Gao, L., Liang, X., Wang, P., and Ma, C. (2021). Palmitoylation of SARS-CoV-2 S protein is essential for viral infectivity. Signal Transduction and Targeted Therapy 2021 6:1 *6*, 1–4. 10.1038/s41392-021-00651-y.
83. Kondo, T., Watanabe, M., and Hatakeyama, S. (2012). TRIM59 interacts with ECSIT and negatively regulates NF-κB and IRF-3/7-mediated signal pathways. Biochem Biophys Res Commun *422*, 501–507. 10.1016/J.BBRC.2012.05.028.
84. Li, S., Wang, L., Berman, M., Kong, Y.Y., and Dorf, M.E. (2011). Mapping a dynamic innate immunity protein interaction network regulating type I interferon production. Immunity *35*, 426–440. 10.1016/J.IMMUNI.2011.06.014.
85. Sui, L., Zhao, Y., Wang, W., Wu, P., Wang, Z., Yu, Y., Hou, Z., Tan, G., and Liu, Q. (2021). SARS-CoV-2 Membrane Protein Inhibits Type I Interferon Production Through Ubiquitin-Mediated Degradation of TBK1. Front Immunol *12*, 1308. 10.3389/FIMMU.2021.662989/BIBTEX.
86. Cao, Z., Xia, H., Rajsbaum, R., Xia, X., Wang, H., and Shi, P.Y. (2021). Ubiquitination of SARS-CoV-2 ORF7a promotes antagonism of interferon response. Cell Mol Immunol *18*, 746–748. 10.1038/S41423-020-00603-6.
87. Buchrieser, J., Dufloo, J., Hubert, M., Monel, B., Planas, D., Rajah, M.M., Planchais, C., Porrot, F., Guivel-Benhassine, F., van der Werf, S., et al. (2020). Syncytia formation by SARS-CoV-2-infected cells. EMBO J *39*. 10.15252/EMBJ.2020106267.
88. Braga, L., Ali, H., Secco, I., Chiavacci, E., Neves, G., Goldhill, D., Penn, R., Jimenez-Guardeño, J.M., Ortega-Prieto, A.M., Bussani, R., et al. (2021). Drugs that inhibit TMEM16 proteins block SARS-CoV-2 spike-induced syncytia. Nature 2021 594:7861 *594*, 88–93. 10.1038/s41586-021-03491-6.
89. Burtscher, J., Cappellano, G., Omori, A., Koshiba, T., and Millet, G.P. (2020). Mitochondria: In the Cross Fire of SARS-CoV-2 and Immunity. iScience *23*. 10.1016/J.ISCI.2020.101631.
90. Hinard, V., Mikhail, C., Pradervand, S., Curie, T., Houtkooper, R.H., Auwerx, J., Franken, P., and Tafti, M. (2012). Key Electrophysiological, Molecular, and Metabolic Signatures of Sleep and Wakefulness Revealed in Primary Cortical Cultures. Journal of Neuroscience *32*, 12506–12517. 10.1523/JNEUROSCI.2306-12.2012.
91. Möller-Levet, C.S., Archer, S.N., Bucca, G., Laing, E.E., Slak, A., Kabiljo, R., Lo, J.C.Y., Santhi, N., von Schantz, M., Smith, C.P., et al. (2013). Effects of insufficient sleep on circadian rhythmicity and expression amplitude of the human blood transcriptome. Proc Natl Acad Sci U S A *110*. 10.1073/PNAS.1217154110.
92. Huber, R., Deboer, T., and Tobler, I. (2000). Effects of sleep deprivation on sleep and sleep EEG in three mouse strains: empirical data and simulations. Brain Res *857*, 8–19. 10.1016/S0006-8993(99)02248-9.

93. Jalili, V., Afgan, E., Gu, Q., Clements, D., Blankenberg, D., Goecks, J., Taylor, J., and Nekrutenko, A. (2020). The Galaxy platform for accessible, reproducible and collaborative biomedical analyses: 2020 update. Nucleic Acids Res *48*, W395–W402. 10.1093/NAR/GKAA434.
94. Kim, D., Paggi, J.M., Park, C., Bennett, C., and Salzberg, S.L. (2019). Graph-based genome alignment and genotyping with HISAT2 and HISAT-genotype. Nat Biotechnol *37*, 907–915. 10.1038/s41587-019-0201-4.
95. Liao, Y., Smyth, G.K., and Shi, W. (2014). FeatureCounts: An efficient general purpose program for assigning sequence reads to genomic features. Bioinformatics *30*, 923–930. 10.1093/bioinformatics/btt656.
96. Ewels, P., Magnusson, M., Lundin, S., and Käller, M. (2016). MultiQC: summarize analysis results for multiple tools and samples in a single report. Bioinformatics *32*, 3047–3048. 10.1093/BIOINFORMATICS/BTW354.
97. Love, M.I., Huber, W., and Anders, S. (2014). Moderated estimation of fold change and dispersion for RNA-seq data with DESeq2. Genome Biol *15*, 550. 10.1186/s13059-014-0550-8.
98. Wu, G., Anafi, R.C., Hughes, M.E., Kornacker, K., and Hogenesch, J.B. (2016). MetaCycle: an integrated R package to evaluate periodicity in large scale data. Bioinformatics *32*, 3351–3353. 10.1093/BIOINFORMATICS/BTW405.
99. Wu, T., Hu, E., Xu, S., Chen, M., Guo, P., Dai, Z., Feng, T., Zhou, L., Tang, W., Zhan, L., et al. (2021). clusterProfiler 4.0: A universal enrichment tool for interpreting omics data. Innovation(China) *2*, 100141. 10.1016/J.XINN.2021.100141/ATTACHMENT/04D49091-826D-4D9D-81C2-4F97B3300FCA/MMC1.PDF.
100. Bindea, G., Mlecnik, B., Hackl, H., Charoentong, P., Tosolini, M., Kirilovsky, A., Fridman, W.H., Pagès, F., Trajanoski, Z., and Galon, J. (2009). ClueGO: a Cytoscape plug-in to decipher functionally grouped gene ontology and pathway annotation networks. Bioinformatics *25*, 1091–1093. 10.1093/BIOINFORMATICS/BTP101.
101. Bindea, G., Galon, J., and Mlecnik, B. (2013). CluePedia Cytoscape plugin: pathway insights using integrated experimental and in silico data. Bioinformatics *29*, 661–663. 10.1093/BIOINFORMATICS/BTT019.
102. Shannon, P., Markiel, A., Ozier, O., Baliga, N.S., Wang, J.T., Ramage, D., Amin, N., Schwikowski, B., and Ideker, T. (2003). Cytoscape: a software environment for integrated models of biomolecular interaction networks. Genome Res *13*, 2498–2504. 10.1101/GR.1239303.
103. Wiese, R., Eiglsperger, M., and Kaufmann, M. (2001). yFiles: Visualization and Automatic Layout of Graphs. Graph Drawing. GD 2001. Lecture Notes in Computer Science (including subseries Lecture Notes in Artificial Intelligence and Lecture Notes in Bioinformatics) *2265 LNCS*, 453–454. 10.1007/3-540-45848-4_42.
104. Kuleshov, M. v., Jones, M.R., Rouillard, A.D., Fernandez, N.F., Duan, Q., Wang, Z., Koplev, S., Jenkins, S.L., Jagodnik, K.M., Lachmann, A., et al. (2016). Enrichr: a comprehensive gene set enrichment analysis web server 2016 update. Nucleic Acids Res *44*, W90–W97. 10.1093/nar/gkw377.
105. Zhang, R., Lahens, N.F., Ballance, H.I., Hughes, M.E., and Hogenesch, J.B. (2014). A circadian gene expression atlas in mammals: Implications for biology and medicine. Proc Natl Acad Sci U S A *111*, 16219–16224. 10.1073/PNAS.1408886111/-/DCSUPPLEMENTAL.

FIGURES + FIGURE LEGENDS

Figure 1

Fig. 1 Acute sleep deprivation profoundly alters the lung transcriptome, dampening the immune system and upregulating pathways involved in viral infectivity. a WT animals were allowed to sleep *ad libitum* (Control) or sleep deprived (SD) between ZT0 – ZT6. Lung tissue was collected at ZT6 and subjected to RNA-sequencing. **b** Of the 18,325 transcripts identified, 4,523 were differentially expressed following SD, with 2,366 upregulated (SD-Up) and 2,157 downregulated (SD-Down). **c** Heatmap of SD differential genes. **d** GO Biological Process (BP) enrichment analysis and term network visualisation, and **e** KEGG pathway enrichment analysis of SD upregulated genes. **f** GO BP enrichment analysis and classification of the SD downregulated terms found that 72% were immune associated, and of these 23% were terms involving adaptive immunity, 18% innate immunity and 31% general immunity. **g** GO BP term network visualisation, and **h** KEGG pathway enrichment analysis of SD downregulated genes. GO BP/functional grouping is indicated by colour, number of terms/genes is indicated by node size, and edges reflect the relationships between the GO BP terms. **i** Normalised RNA-sequencing counts of *Ccl5*, *Tnf*, *Il6* and *Ifng* (grey – control, red – 6h sleep deprivation). **j** Protein concentration of CCL5, TNF-α, IL-6 and IFN-γ as determined by ELISA (grey – control, red – 6h sleep deprivation). **k** Volcano plot of the significantly differential genes following SD. SD-Up (red) and SD-Down (blue) genes are highlighted, with genes in grey being non-significant. For **c** data are Z-score normalised per row and for **j** and **i** data are mean $\pm$ SEM. n=5-16. Statistical analysis of RNA sequencing data was conducted using DESeq2, and genes with a BH adjusted p value of < 0.05 were considered significant. For **j** and **k** statistical analysis was conducted by two-way ANOVA with Sidak's multiple comparisons correction. ns $p > 0.05$, * $p < 0.05$, *** $p < 0.001$.

Figure 2

Fig. 2 Acute sleep deprivation leads to dysregulation of the circadian system in the lung. WT animals were stably entrained to a 12:12 LD cycle, and then placed into constant darkness. Lung samples were then collected at CT2, CT8, CT14 and CT20 and RNA sequencing conducted. **a** Heatmap of the 2,029 significantly cycling genes in the lung. **b** A comparison with genes differentially expressed following SD with the lung circadian genes found 991 rhythmic genes that were also disrupted by SD. Network visualisation of the significantly enriched GO BP terms of the **c** 3,532 genes that are non-cyclic in the mouse lung, but disrupted by SD (green), and **d** the 991 genes that are cycling in the mouse lung and disrupted by SD (blue). Each node represents a GO BP term. Related terms are grouped by colour and edges reflect the relationship between them. **e** RNA sequencing counts of core circadian clock genes in the control and SD lung samples. **f** PCA projection of the circadian (CT) samples in the PC space determined from 10 known circadian transcripts. The black spline represents the estimated circadian behaviour of mouse lung under constant conditions, and the graph is oriented such that the separation between the CT samples is as clear as possible. The control samples (black crosses) projected near to the black spline at the approximate expected location, however the SD samples (red crosses) did not project to the same location, demonstrating that SD resulted in circadian disruption in the lung. **g** A Support Vector Machine (SVM) approach with the linear kernel was used to find the plane which optimally separated the control and SD samples in the 3D principal component space. The samples were projected onto the normal of this plane, and a clear separation between the two groups can be seen, which was statistically significant (Wilcoxon rank sum test – $p = 0.0022$). Therefore, SD results in circadian disruption of the lung transcriptome. For **a** data are Z-score normalised per row and for **e** data are mean ± SEM. n=5-6. Cycling genes were determined using MetaCycle, and genes with a BH corrected q value of < 0.05 were considered as significantly rhythmic. For **f** and **g** statistical analysis was conducted using the Wilcoxon rank sum test.

Figure 3

Fig. 3 Critical host factors that interact with SARS-CoV-2, and are needed for infection, are differentially expressed in the mouse lung after sleep deprivation. a-**c** Venn diagrams of the overlap between all SD differential genes in the mouse lung and critical host factors for viral infection as determined by **a** Daniloski *et al*. (2021), **b** Zhu *et al*. (2021), and **c** Wei *et al*. (2021). **d** Volcano plot of significant SD differential genes (Up – red, Down – blue and non-significant after BH p value correction – grey) with overlapping critical host factors highlighted (purple diamonds) and a subset labelled. **e** The intersection between SD differential genes in the mouse lung and the SARS-CoV-2-human protein interactome as determined by Gordon *et al*. (2020b). **f** Volcano plot of SD differential genes with overlapping SARS-CoV-2-human protein interactors highlighted (yellow diamonds) and a subset labelled. **g** Functional classification of the critical host factors and the SARS-CoV-2-human protein interactors that were found to be differentially expressed in the mouse lung following SD. Boxes are coloured according to the functional role in viral infectivity. Statistical significance of the overlap between SD differential genes and SARS-CoV-2 host factors and host interactome was assessed by two-tailed Fisher's exact test. n=5-6. ERGIC = endoplasmic reticulum-Golgi apparatus intermediate compartment.

Figure 4

Fig. 4 Involvement of differentially expressed genes after sleep deprivation in the SARS-CoV-2 life cycle. (**1**) SARS-CoV-2 binds ACE2 and enters via endocytosis or membrane fusion, depending on the availability of TMPRSS2/4. (**2**) The viral RNA genome is released into the cytoplasm and (**3**-**4**) replicated and (**5**) transcribed by RdRp. (**6**) Viral structural proteins are translated by host ribosomes. (**7**-**8**) The virion assembles and (**9**) is released. All differentially expressed genes shown (red font for SD-Up, blue font for SD-Down) apart from *FURIN, TMPRSS4, GSK3A, SRPK1*, and *CSNK1A1* are critical host factors overlapping with at least one of the studies from Gordon *et al*. (2020b), Daniloski *et al*. (2021), Wei *et al*. (2021), or Zhu *et al*. (2021). Drugs targeting SD differential or viral genes mentioned are in green font. Cycling genes are denoted by a yellow clock. ACE2 = angiotensin-converting enzyme 2, ERGIC = ER-Golgi apparatus intermediate compartment, RdRp = RNA-dependent RNA polymerase, TMPRSS2 = transmembrane protease serine 2. Adapted from Du *et al.* (2009) and from “Coronavirus Replication Cycle” by BioRender.com. Created with BioRender.com.

Figure 5

Fig. 5 The effect of sleep deprivation on the anti-SARS-CoV-2 immune response and viral immune evasion. (**1**) The virus enters the host cell. Viral RNA is detected by (**2**) endosomal TLRs or (**3**) cytosolic RIG-I and MDA5, which activate MAVS. (**4**) Both recognition events activate NF-κB and IRFs, which (**5**) translocate into the nucleus to (**6**) drive the expression of IFNs and inflammatory cytokines to amplify the antiviral immune program, for example by priming dendritic cells to sample and display viral antigens to (**7**) activate naive $CD8^+$ T cells. Inside the infected host cell, (**A**) viral material is broken down and displayed on the cell surface by MHC class I molecules. If the antigen is recognised by $CD8^+$ T cells (**B**) it induces apoptosis of the infected host cell. All differentially expressed genes shown (red font for SD-Up, blue font for SD-Down) are involved in the acute innate immune response against SARS-CoV-2. Genes in green-shaded text boxes are implicated in viral immune evasion, as described in Gordon *et al*., (2020b). IFN = interferon, IRF = interferon regulatory factor, MAVS = mitochondrial antiviral signalling protein, MDA5 = melanoma differentiation-associated protein 5, MHC I = major histocompatibility complex molecule class I, NF-κB = nuclear factor kappa B, RIG-I = retinoic acid-inducible gene 1. Adapted from "Acute Immune Responses to Coronaviruses", by BioRender.com. Created with BioRender.com.

Supplementary Table 1. RNA sequencing and differential gene expression analysis of Control and SD lung. Related to Figure 1.

Supplementary Table 2. GO BP and KEGG enrichment analysis of SD differential genes. Related to Figure 1.

Supplementary Table 3. Gene set enrichment analysis (GSEA) of SD differential genes using the COVID-19 Drug and Gene Set Library. Related to Figure 3.

Supplementary Table 4. Overlapping gene/protein lists with our SD differential genes.Related to Figure 3.

Supplementary Table 5. Transcription factor enrichment analysis of the SD significantly differential transcripts using Enrichr. Related to Figure 1.

Supplementary Table 6. Metacycle analysis of lung time course RNA sequencing. Related to Figure 2.

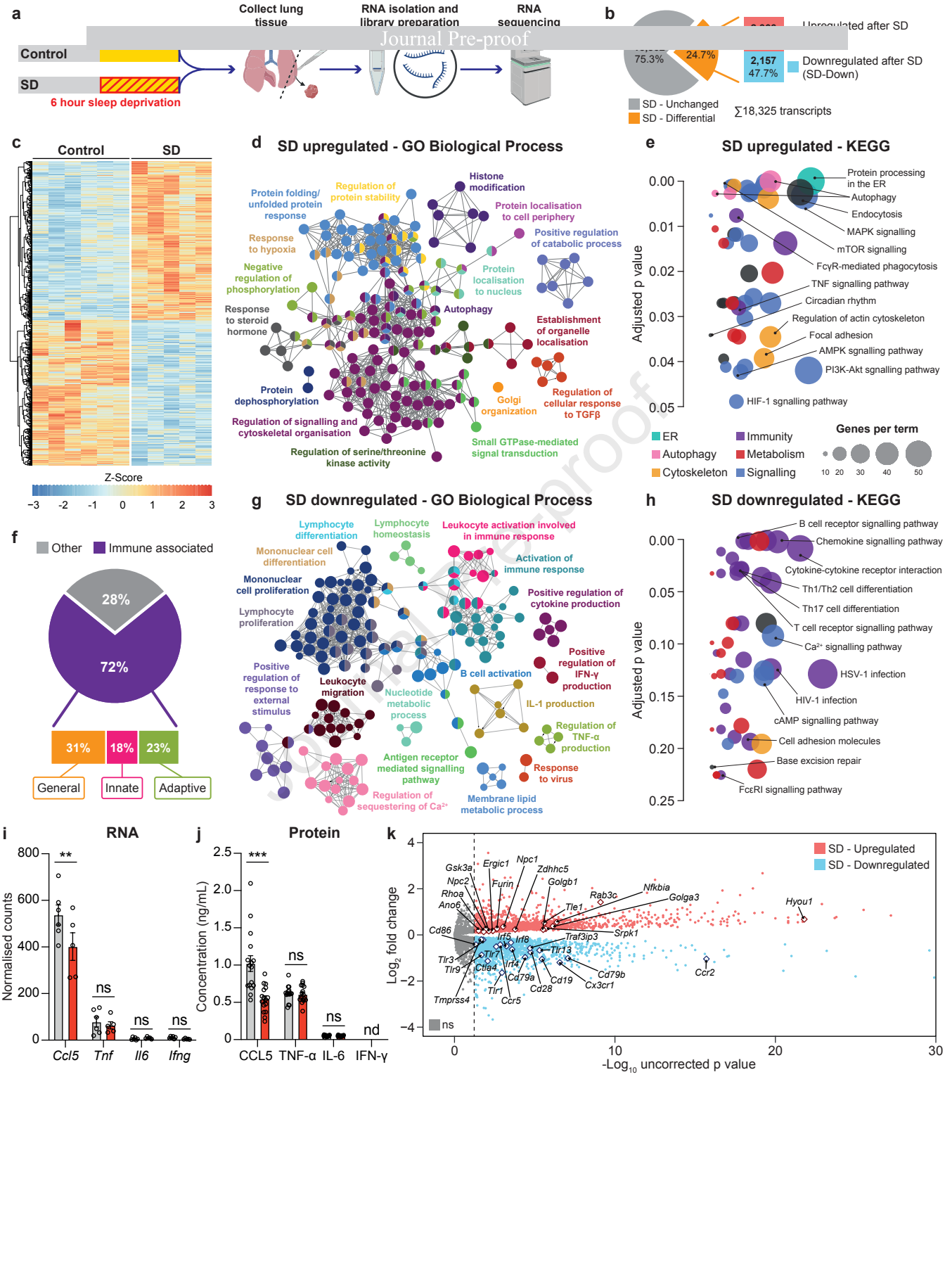

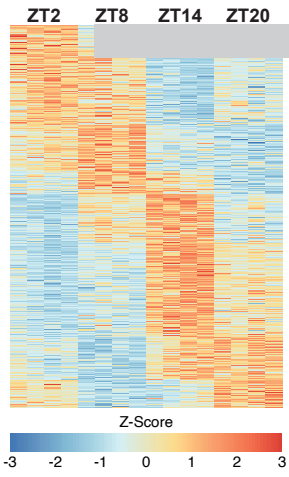

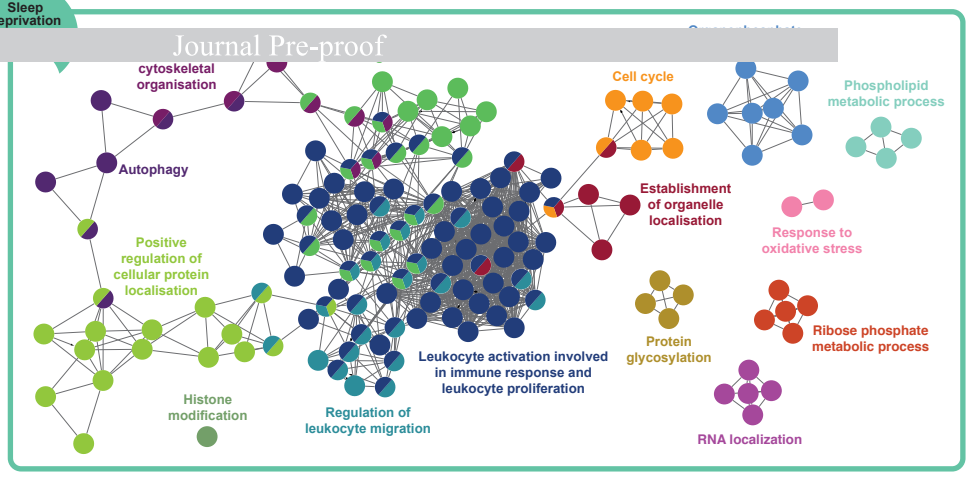

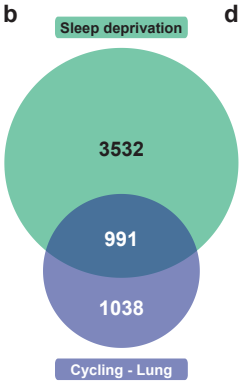

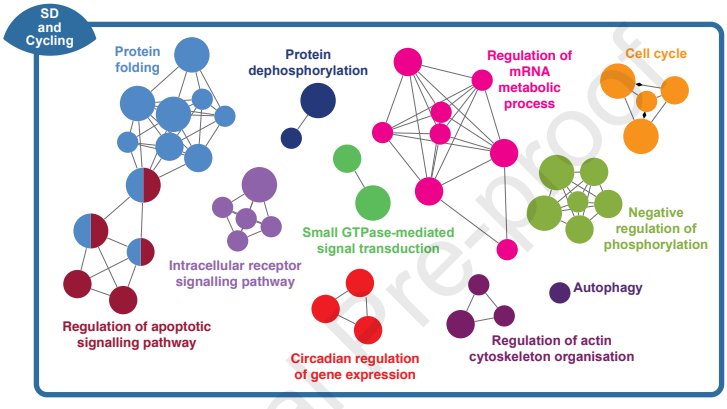

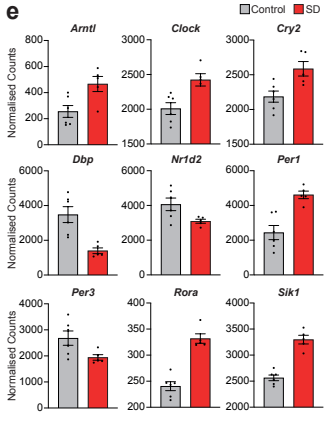

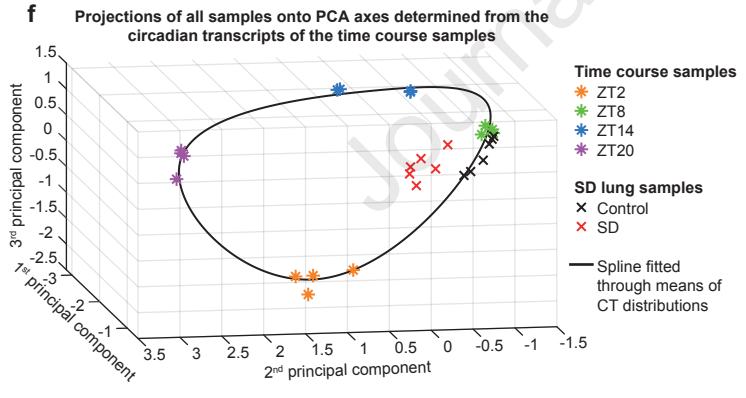

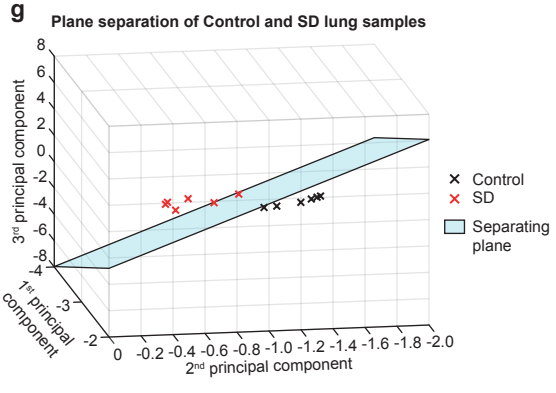

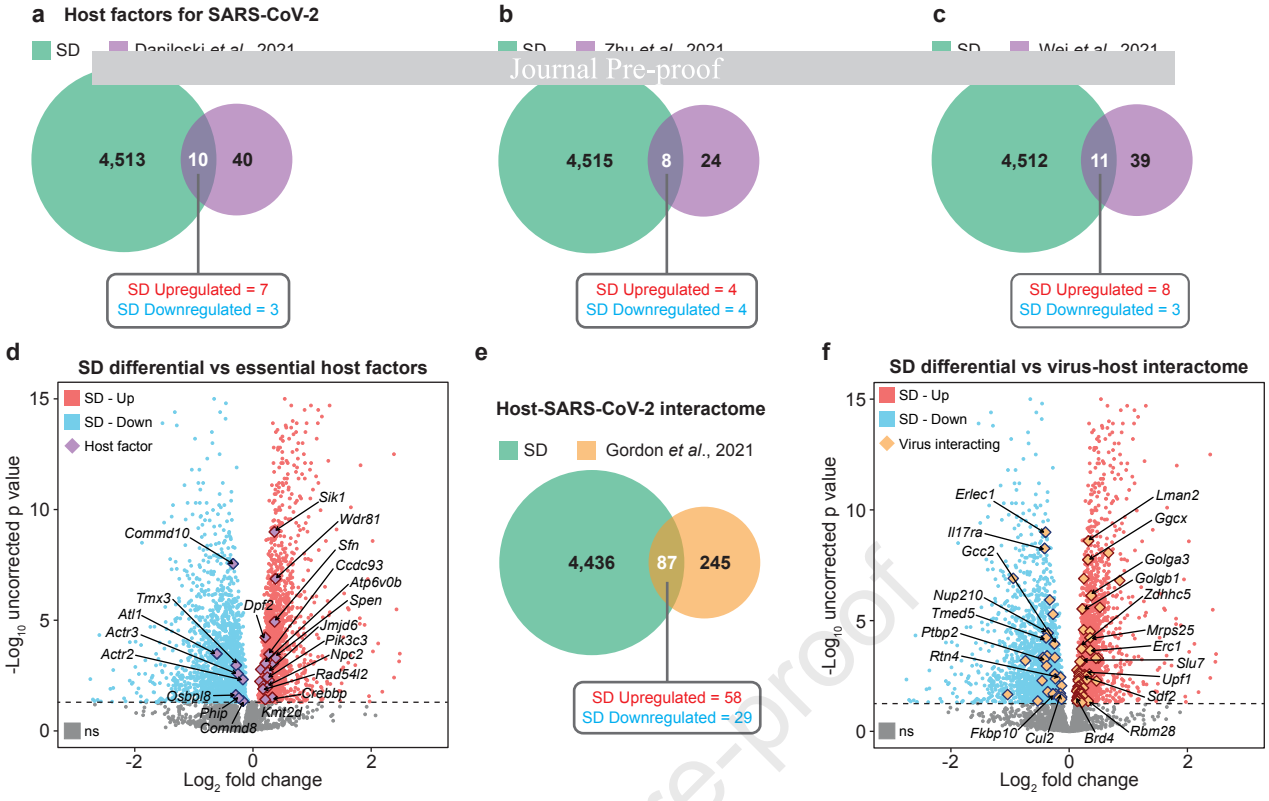

g

SD - Down
SD - UP

SARS-CoV-2 life cycle

RNA Processing
CWC27, PTBP2
CSDE1, EIF4H, JMJD6, RBM28, SLU7, UPF1

Transcription
CREBB, PCRTC3, DPF2, ELOA, MEPCE, RAD54L2, SPEN

Palmitoylation
ZDHHC5

Cholesterol homeostasis
OSBPL8, TEME97
NPC1, NPC2

Endoplasmic reticulum
ERLEC1, FKBP10, RTN4, SRP72
GGCX, HYOU1, MOGS, SDF2, POGLUT2, POGLUT3, WFS1

Golgi & ERGIC
ATL1, GCC2, TMED5
AP3B1, ERGIC1, GCC1, GOLGA3, GOLGB1

Trafficking
ACTR2, ACTR3,COMMD8, COMMD10, NUP210, RAB14
AP2M1, ATP6AP1, ATP6V0B, ATP6V0D1, FKBP15, LMAN2, WDR81

SARS-CoV-2 immune evasion

Immune regulation
G3BP2, IL17RA
ERC1, PVR, RIPK1, TBKP1, TLE1

Mitochrondria
DNAJC19
ATP1B1, DNAJC11, MRPS25, TIMM29

Ubiquitylation
CUL2, TRIM59, USP13
MIB1, RNF41, USP54

Other biological functions

Coagulation
ANO6, PLAT

Signalling
PHIP, TMX3
COMT, GNB1, MARK2, PIK3C3, PLEKHA5, PRKAR2A, RAP1GDS1, RHOA, SFN, SIK1

Epigenetic
BRD4, KMT2D, NSD2, RYBP

Other functions
CEP43, CHPF2, HS2ST1, HS6ST2, JAKMIP1, NIN, PPT1, PUSL1, SCCPDH, SMOC1, TUBGCP2
LOX, NAT14, NPTX1, PCNT, PRRC2B, RETREG3, SLC30A9, SUN2, UBAP2L, ZC3H18

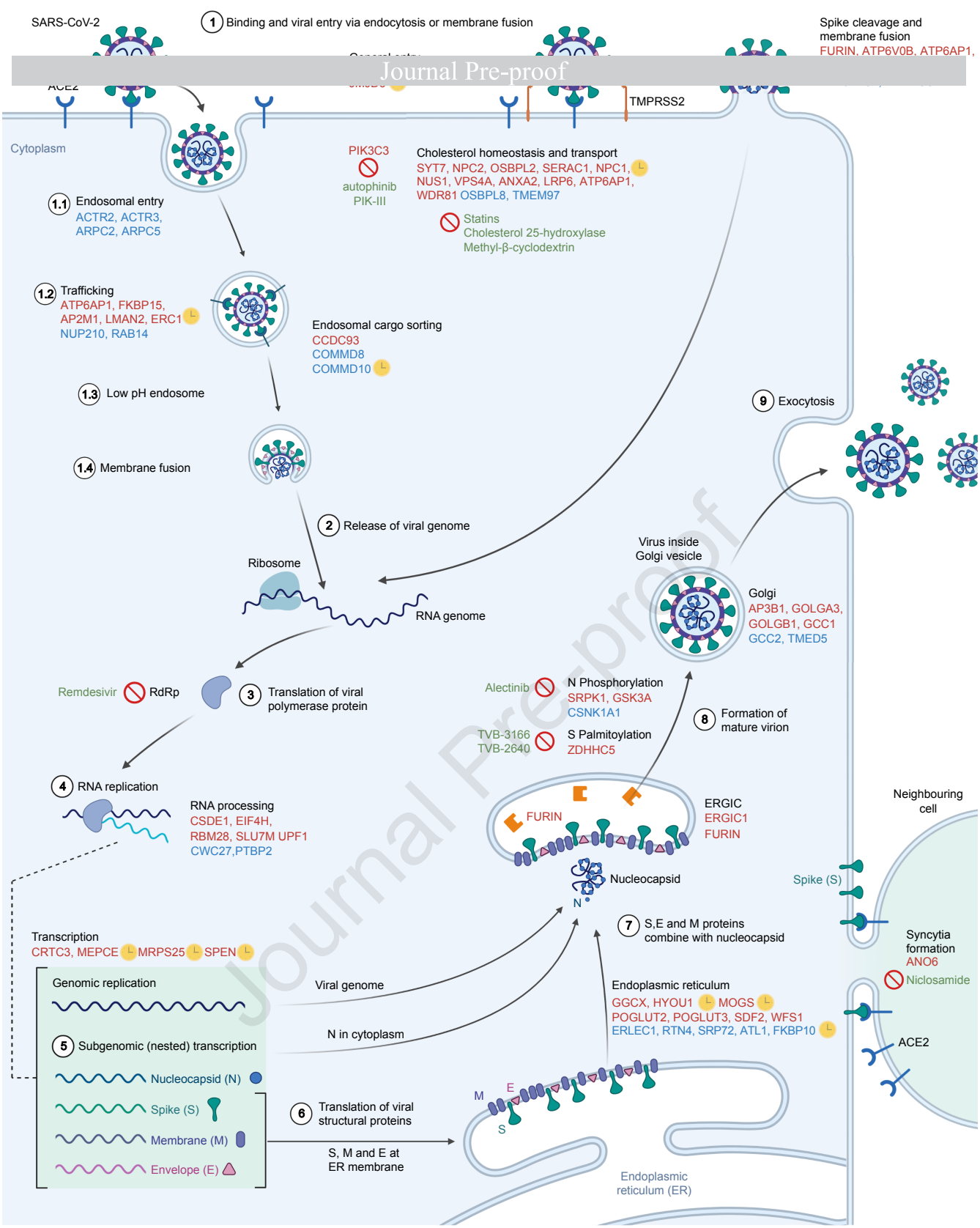

Legend

ACE2 · TMPRSS2 · FURIN · Nucleocapsid (N) · Spike (S) · Membrane (M) · Envelope (E) · Rhythmic · SD - Up · SD - Down · Inhibitor

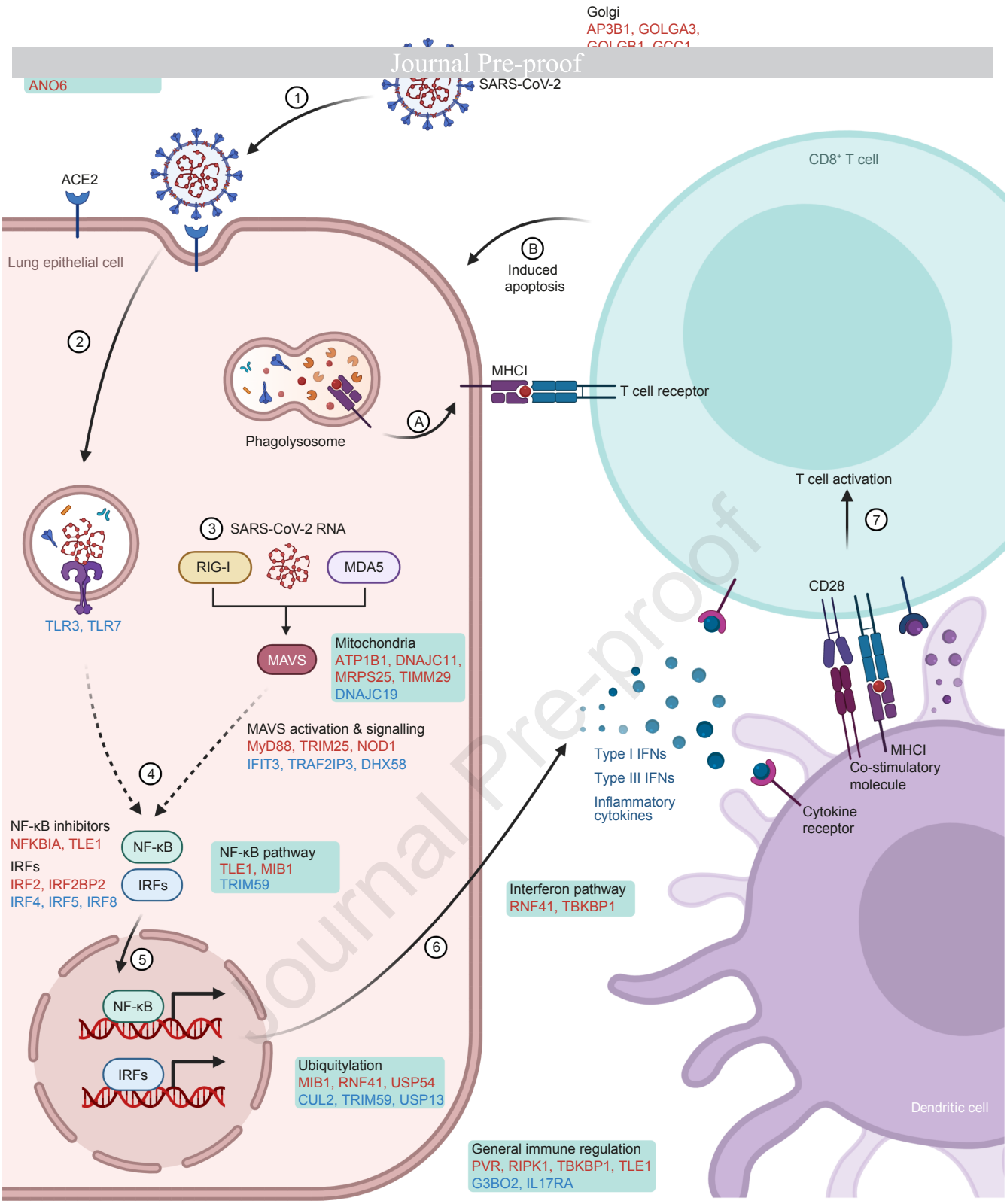

Legend

Spike protein · Nucleocapsid protein · Protease · Cytokine/IFN · CD28 · T cell receptor · SD - Up · SD - Down

Envelope protein · Membrane protein · Viral RNA · Cytokine receptor · Co-stimulatory receptor · Antigen · MHCI · Gene implicated in immune evasion

Taylor et al.

Highlights

1) Sleep disruption alters the mouse lung transcriptome
2) This results in supressed innate and adaptive immune systems
3) The changes are driven by a disrupted circadian clock
4) This generates a lung environment that would promote viral infection